

NAT'L INST. OF STAND & TECH R.I.C.



A11104 232683

NATIONAL INSTITUTE OF STANDARDS &
TECHNOLOGY
Research Information Center
Gaithersburg, MD 20899

IR 88-3730

RESTRICTED

NBSIR 88-3731

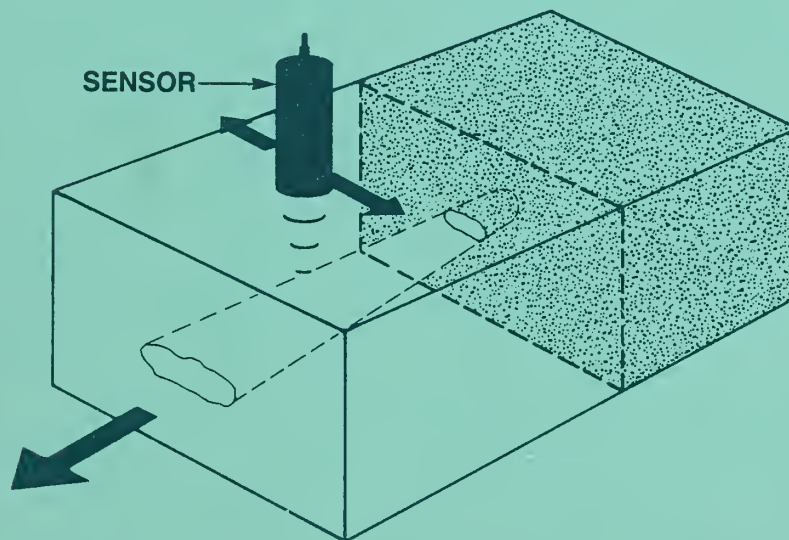
Internal Discontinuity Sensor Needs for Steel

Report of Workshop

July 16, 1986

Edited by

H. N. G. Wadley and C. D. Rogers



Sponsored by

American Iron and Steel Institute
National Bureau of Standards

Hosted by

U. S. Department of Commerce
National Bureau of Standards
Institute for Materials Science and Engineering
Gaithersburg, MD 20899



June 1988



NBSIR 88-3731

Internal Discontinuity Sensor Needs for Steel

Report of Workshop

Edited by
H. N. G. Wadley and C. D. Rogers
July 16, 1986

Sponsored by

American Iron and Steel Institute
National Bureau of Standards

Hosted by

U. S. Department of Commerce
National Bureau of Standards
Institute for Materials Science and Engineering
Gaithersburg, MD 20899

June 1988



U.S. DEPARTMENT OF COMMERCE, C. William Verity, *Secretary*
NATIONAL BUREAU OF STANDARDS, Ernest Ambler, *Director*



A need has emerged for online detection of internal discontinuities during continuous casting of steel. Sensing of these defects is generally considered beyond the sensitivity of existing instrumentation and probably requires a focused research effort. A workshop was convened on July 16, 1986 at the National Bureau of Standards to assess the status of emerging sensor technologies and to explore the feasibility of internal discontinuity detection at various stages during the processing of steel. This report summarizes the presentations and conclusions of the workshop.

We wish to express our gratitude to J. R. Cook, W. Wilson, M. Linzer and R. B. Clough for helping to organize and run the workshop and to the speakers whose presentations provided excellent background and stimulus for subsequent working group discussions. We would like to also thank Dr. William E. Dennis of the American Iron and Steel Institute who provided encouragement and helpful advice for this activity. Finally, we are indebted to Antonette Nashwinter for assisting in organizing the program and preparing this report for publication.

TABLE OF CONTENTS

1. Introduction	1
2. Formal Presentations	3
Process Control Sensors: Status of AISI Collaborative Programs H. N. G. Wadley, <i>National Bureau of Standards</i>	5
Recent Progress in the Evaluation of a Pipe/Porosity Sensor D. Kupperman, <i>Argonne National Laboratory</i>	23
A Pulsed Laser/Electromagnetic Acoustic Transducer Approach to Ultrasonic Sensor Needs for Steel Processing G. A. Alers, <i>Magnasonics, Inc.</i>	27
Non-Contact Laser Ultrasonic System for Inspection of Hot Steel Bodies During Processing M. Rosen and R. E. Green, <i>Johns Hopkins University</i>	39
Impedance of a Coil in the Vicinity of a Crack A. H. Kahn, <i>National Bureau of Standards</i>	51
3. Workshop Summaries	59
3.1 Solidification	59
3.2 Intermediate Forming	63
3.3 Finishing	64

SUMMARY AND RECOMMENDATIONS

Operators, engineers and researchers representing American Iron and Steel Institute member companies met with scientists and engineers from federal laboratories, universities, and sensor vendor companies to:

- Determine the formation mechanisms of internal discontinuities in continuous cast steel and their effect on steel quality.
- Identify potential online sensor technologies for internal discontinuity detection and control strategies for their elimination.

During formal sessions, the Workshop addressed the status of many emerging sensor technologies with the potential to detect online, internal discontinuities in steel. During informal workshops, working groups then convened to discuss the types and origin of discontinuities observed during:

- Solidification
- Intermediate forming
- Finishing

The working groups identified and prioritized the important defects, assessed the potential of emerging sensor methodologies for their detection and identified research and development needs.

Steel industry representatives concluded that the top priority problem was the elimination of surface/subsurface cracks and inclusions. These almost always originate in the continuous caster. As cast material undergoes subsequent rolling/drawing, many of these anomalies result in surface cracks that are harmful both to quality and productivity. A second priority was sensing the occurrence of center line segregation/center looseness. The consensus viewpoint was that each of these defect types could be eliminated from steel product by adjustment of the continuous caster, provided online sensors were able to indicate the movement of their formation. The alternative solution of cropping and discarding unsound material after offline cold inspection was considered a less desirable expedient because of the loss of yield and the long time lag before detection of faulty processing conditions in the caster. While significant strides in statistical process control and other quality management programs have been made, offline control scenarios do not allow timely enough detection of internal discontinuities.

The development of online sensors to detect inclusions and cracks within the caster was determined to be urgently needed for real time quality

control. Outputs from such sensors could be used to detect inert gas shroud failures (the most common source of the most deleterious inclusions) and cracking problems and facilitate feedback control. Of all the potential sensor methodologies addressed, ultrasonic approaches similar to those developed for porosity work and also related to those under development for internal temperature/solidification interface measurement were considered the most promising. Collaborative programs need to be instituted to prove the ultrasonic approach and to develop data for the design of a prototype sensor.

1. INTRODUCTION

A Briefing/Workshop on Internal Discontinuity Sensor Needs for Steel was convened and attended by 50 people on July 16, 1986 at the National Bureau of Standards, Gaithersburg, Maryland. It was sponsored by the American Iron and Steel Institute (AISI) and the National Bureau of Standards (NBS). The aims of the Briefing/Workshop were first to provide scientists and engineers in industry, universities and government with the specific needs of sensors for detecting online the formation of internal discontinuities in steel, and second, to seek immediate input and future research and development involvement from a broad spectrum of disciplines to facilitate sensor development. This report is the proceedings of the presentations and deliberations from the Briefing/Workshop.

The General Research Committee of AISI has identified the development of Process Control Sensors as an area of research that would have substantial impact toward improving both productivity and quality in the steel industry. A January 1981 draft report entitled "Steel Industry Priorities for Process Control and Sensor Development" identified 537 process control sensor needs spanning 35 steel processes. A Briefing/Workshop in July, 1982 addressed in detail four of the sensor needs.

- Automatic detection of pipe and gross porosity in hot steel billets, blooms or slabs.
- Online inspection of surface defects on hot and cold strip.
- Rapid in-process analysis of molten metal.
- Rapid measurement of temperature distribution within a solid or solidifying body of hot steel.

Following the workshop, research programs involving cooperation between AISI member companies, federal laboratories, universities and vendor companies were initiated for each sensor. These programs are now reaching the stage of prototype installation (see following summaries in section 2) and evaluation.

The furthest advanced sensor is that for the automatic detection of pipe and porosity. An ultrasonic approach has been developed at NBS/Magnaflux and successfully evaluated at the Argonne National Laboratory (A.N.L.) using a contact technique. While this contact method of hot ultrasonic inspection provides an interim (pragmatic) solution to this sensor need, it has been recognized that ultimately a noncontact system would be preferred. Noncontact ultrasonic inspection approaches based upon high intensity lasers/electromagnetic acoustic transduction are beginning to emerge now

from the laboratory, and the time may well be right for exploring their application to the pipe/porosity sensor need.

Concomitant with this has been the increasing awareness of sensor needs for detecting smaller internal discontinuities such as cracks, inclusions and center-line segregation which lead to significant reductions in productivity. Could a modified version of the internal pipe/porosity sensor potentially meet these other needs? If so, there would be considerable merit in developing a coordinated research/development program for a more general internal discontinuity sensor. The avoidance of duplicated effort, and the much larger potential market for the generic sensor, would enhance the cost/risk ratio to the point where a commercial device might emerge from the sensor vendor industry.

To this objective, a Workshop/Briefing was convened at the National Bureau of Standards in July 1986. Operators, engineers and research technologists representing AISI member steel companies met with researchers from university, government and vendor companies to:

- Identify the most important internal discontinuities and their point of origination during processing.
- Review candidate sensor methodologies, and suggest promising research/development directions.
- Encourage the development of a research/development consortium to pursue development of a sensor.

This report summarizes the proceedings of the meeting.

2. FORMAL PRESENTATIONS

PROCESS CONTROL SENSORS: STATUS OF AISI COLLABORATIVE PROGRAMS

H. N. G. WADLEY

Institute for Materials Science and Engineering
National Bureau of Standards
Gaithersburg, MD 20899

INTRODUCTION

The American Iron and Steel Institute (AISI) is presently engaged in several collaborative research programs whose objective is the development of process control sensors. These sensors are complex systems based upon the sophisticated application of advanced technologies featuring high intensity lasers, ultrasound propagation, high speed digital data acquisition and signal processing. No single steel industry research laboratory has the resources to tackle these multidisciplinary research programs. In view of this, these programs feature an unusual level of cooperation. Cooperation exists between individual AISI member companies metals industries concerned with other metals such as aluminum, and extends to several federal laboratories, universities and vendor companies. As these programs begin to establish varying degrees of feasibility for the proposed sensor technologies, and the first tangible benefits (prototype sensors) begin to emerge and undergo industry evaluation, it is opportune to discuss the factors that led to their conception, development and present status, and to address the future directions that these programs may take.

HISTORICAL BACKGROUND

The AISI Sensor Programs were conceived in 1979 when the General Research Committee of AISI identified the development of process control sensors as an area of research that would substantially impact productivity and quality in the steel industry. On March 11, 1980, the General Research Committee directed the establishment of a Task Group to formulate a plan of research and development relevant to the process control and sensor needs of the steel industry. The purpose of this group was to develop a framework within which discussion with appropriate organizations could begin and basic sensor research and development could be started. The Task Group had very broad industry participation and included representatives from thirteen AISI member companies.

On January 8, 1981, the Task Group issued a draft report entitled "Steel Industry Research Priorities for Process Control and Sensor Development" (Ref. 1). In this report, the Task Group critically evaluated sensor applications and identified sensor needs across the entire steel industry. In the analysis, 35 steel processes were studied, and a total of 537 sensor needs identified. Approximately 70% of the

sensors were for applications involving closed- or open-loop control systems. The majority of the remainder were for periodic monitoring applications, with a small remaining percentage needed for research techniques.

The Task Group assessed the sensor needs and reached the following conclusions:

- 40% of the sensor needs could be met adequately with commercially available equipment.
- 25% of the needs could be partially satisfied with existing equipment.
- 25% of the sensor needs had well established measurement methodologies but no commercially available equipment.
- 10% of the sensor needs did not have established measurement principles.

The latter two categories were considered potential candidates for collaborative research programs.

Individual member companies were asked to evaluate these two categories of needs with respect to present availability, level of interest, and their significance both for current and proposed future operations. This ranking process reduced the number of research needs to a list of 18 potential process control sensors that were then considered, on an industry wide basis, to be the most significant.

From this list of 18 sensors, the AISI assigned top priority to four specific sensors:

- Rapid In-Process Analysis of Molten Metal.
- Online Inspection for Surface Defects on Hot and Cold Strip.
- Automatic Detection of Pipe and Gross Porosity in Hot Steel, Billets, Blooms or Slabs.
- Rapid Measurement of Temperature Distribution within a Solid or Solidifying Body of Hot Steel.

In August 1981, task force units were established for each sensor. These units were composed of senior scientists and engineers from member companies and were assigned responsibility for initiating research programs that ultimately would lead to the development of a sensor and associated analysis methods.

Each task force unit prepared a detailed research prospectus identifying intended applications for the sensor, benefits of such a sensor to the domestic

industry, detailed sensor specifications, and a description of the environment in which the sensor would be required to operate.

On July 27-28, 1982, a workshop was convened at the National Bureau of Standards to highlight these four sensor needs (Ref. 2). Presentations by steel industry research staff were made to a wide range of government, university and industry researchers and were followed by working group sessions convened to evaluate candidate sensor methodologies. The Workshop concluded with a request from each of the task force units for research and development proposals from qualified organizations.

Each task force unit subsequently evaluated all of the proposals received and developed a research program that, in some cases, involved teaming of proposals. These research prospectuses were circulated to member steel companies and other organizations with a shared interest in the research. Individual companies then grouped together to collaboratively fund the various research programs. Further cofunding was negotiated with other interested organizations such as the U.S. Department of Energy (DOE) and the National Bureau of Standards (NBS). Contracts and cooperative agreements were then signed and the research initiated.

A very important aspect of the research and development to date has been the development of mechanisms for continued day-to-day involvement of steel industry research staff with each of the research programs. This has taken many forms, including frequent program reviews, site visits, and of particular importance to several of the programs, the extended reassignment of industry research staff to various laboratories to participate in the research itself. This, together with detailed reporting, has contributed greatly to the success of the technology transfer process.

RAPID INPROCESS ANALYSIS OF MOLTEN METAL

The objective of this program is the development of a sensor for the rapid in-process chemical analysis of liquid metal and alloys. The sensor is required to measure only the metal composition and not to sample oxidation products, slag or furnace refractory materials. It must be capable of a rapid multielement readout (<1 minute), operate without interference to normal liquid metal processing and to be sufficiently robust to withstand the extremely hostile environment of a blast furnace or refining facility.

The sensor was envisaged to have numerous potential applications in a steel mill including:

- Continuous iron composition measurement during blast furnace operation.
- Rapid steel analysis during refining processes.

- Sulfur content measurement during iron and steel desulfurization processing.
- Control of ladle treatments.
- Control of composition at the top of a continuous caster and optimization of alloy additions during vacuum degassing.

Other unspecified uses/benefits were anticipated for the nonferrous metals industries, which encouraged development of a generic approach.

The anticipated benefits to the steel industry of these inprocess analysis sensors are very substantial. For example, in 1982, their implementation would yield \$200 million of potential savings from:

- Reduction of heat time. Inprocess chemical analysis would lead to substantial time savings of 3-7 minutes in heat time during both oxygen and electric furnace steelmaking thus both improving productivity (through additional heats in the available time) and reducing operating costs (by enabling the same number of heats in less time).
- Increase of refractory life. The reduction of heat time would reduce the length of time that corrosive, end-of-melt slag would be in contact with refractory linings.
- Reduction of materials costs. Closer composition control during refining would lead to savings in oxygen, aluminum, flux, and ferro-alloys.
- Reduction of desulfurization costs. Inprocess sulfur analysis during desulfurization would verify effective removal of sulfur and eliminate costly and time consuming overtreatment.

The use of inprocess analysis sensors would also reduce the incidence of overblown heats, and enable better attainment of customer specifications and better quality.

The task force unit evaluated numerous potential approaches and candidate technologies for an inprocess chemical analysis sensor. These included a variety of emission spectroscopy techniques coupled with laser ablation/aerosol sampling of the melt and nuclear activation techniques. The approach considered most promising was the combination of laser ablation as a means of sampling, coupled with emission spectroscopy as a method of analysis.

In this approach, an intense laser pulse was envisioned as a method to heat, vaporize and electronically excite the atomic species present in liquid metal. The plasma so created would then decay by the emission of photons of frequency characteristic of the atomic species. By measuring the intensity of particular

frequencies in the emitted spectrum, a measurement of the concentration of each element could be obtained.

In 1983, a cooperative research program began at the DOE's Los Alamos Laboratory to explore the use of pulsed lasers for the production of representative plasmas - the first prerequisite for implementation of the laser approach. This work showed that when pulsed lasers with moderate power density are used to cause surface ablation, preferential vaporization of volatile elements occurs. This results in an overabundance of emission from volatile elements in the emission spectrum and hence a potentially serious inaccuracy in determined composition.

However, researchers at Lehigh University applied plasma transport theory to model the plasma formation process at alloy surfaces and have found that it is theoretically possible to overcome this sampling problem and attain complete vaporization (of all atomic species regardless of volatility) by operating in a specific pulse energy density/pulse duration domain. This has led to the recent implementation of a new program centered at Lehigh University under the leadership of Professor Y. Kim. The program began in late 1985 and is aiming to develop a mill-worthy prototype within two years.

The budget for this program exceeds \$0.5 million and is supported by a Consortium of AISI member companies (including two from Canada), one aluminum producer and the Ben Franklin Foundation. There is also close collaboration with a related program underway in the Center for Metals Production at the Mellon Institute.

ONLINE INSPECTION FOR SURFACE DEFECTS ON HOT AND COLD STRIP

The objective of this program is the inprocess detection, characterization and classification of surface defects on hot or cold strip steel so that inprocess control can be used to enhance quality. In order to achieve this objective, the sensor would have to:

- Have a high speed capability commensurate with strip speeds up to 5,000 feet per minute (posing serious problems for data acquisition and analysis with present commercially available systems).
- Be capable of defect classification and the separation of significant defects and spurious indications (e.g., rolling solution droplet).
- Have a high reliability in the harsh rolling-mill environment.

It was envisioned that a successfully developed sensor would be used in hot strip mills, pickle lines, tandem mills, temper mills, and online inspection operations. Its potential benefits would include:

- Early identification of problems in processing which produce defects, facilitating their prevention at source.
- Elimination of costly reprocessing of defective material.
- Reduction of manpower presently required for visual inspection.
- Elimination of production delays caused by present slow manual inspection methods and the need for reinspection.
- Improvement of quality of shipped material.
- Provision of extensive documented information in digital form confirming an overall high level of consistent quality together with the exact location of isolated defects.

These anticipated benefits were estimated in 1982 to be potentially capable of annual savings of \$50 million in the domestic steel industry. The improvement in quality and consistency could also be very important factors in the international marketplace. Furthermore, the sensor was recognized to have potential for similar inspection and control needs in the nonferrous metals industry.

Technical approaches proposed to the task force unit included the use of eddy current techniques, ultrasonics and optical scattering. The unit determined that the optical scattering approach was the most promising for surface inspection. It was recognized, however, that future subsurface defect inspection needs might incorporate eddy current and/or ultrasonic technologies.

On July 15, 1984, a contract was signed with the Westinghouse Corporation for phase I of a three phase sensor development program based on an optical scattering approach. The initial contract was for a two year study of feasibility and development of prototype technical specifications. The research budget was entirely funded by a group of eleven steel and aluminum companies under AISI auspices.

The technical approach being pursued at Westinghouse is a coherent light scattering approach, shown schematically in Fig. 1. An intense collimated laser beam is rapidly scanned across the width of the moving metal strip. Detector arrays are positioned across the strip width at angles predetermined to optimize the defect scattering (signal) to background scattering (noise) ratio. The detector outputs are digitized and processed, the processed information stored, and the presence of defects appropriately indicated.

Technical issues that are being addressed include a variety of strategies designed to maximize the signal-to-noise ratio (contrast) of important defects, cataloging the characteristic features (signatures) of both defects and spurious indications for characterization purposes, developing very high speed data

acquisition systems, designing and evaluating data reduction schemes and developing software so that true defects may be discriminated from spurious events and the defects characterized. The ultimate objective is a full mapping and characterization of all surface defects in excess of 0.8 mm.

An extensive contrast ratio data base has been compiled for numerous defects on a wide product range. Techniques being developed to address the defect recognition problem can be classified as one of three types:

- Implementation of measurement techniques that are minimally sensitive to false defects.
- Use of additional synchronized measurement systems that locate only the false defects, for example, drops of rolling solution.
- Development of advanced pattern recognition software that recognizes the characteristic signatures of defects and classifies them.

Even though the first two approaches are likely to filter out many of the false defects, some are likely to remain, and advanced software will be necessary to recognize the signatures of these false defects and to classify the true defects.

Progress to date has been sufficiently encouraging that a test facility is being prepared on a strip mill at the Weirton Steel Corporation Works in Weirton, West Virginia. This facility will be used to gather information, gain experience of mill operating conditions, and to perform tests on a range of product containing carefully documented defects. For this latter purpose, an extensive inventory of representative defects has been obtained from participating steel and aluminum companies. This study is presently anticipated to lead to the construction and installation of a full prototype system for mill evaluation within two years.

RAPID MEASUREMENT OF TEMPERATURE DISTRIBUTION WITHIN A SOLIDIFIED OR SOLIDIFYING BODY OF HOT STEEL

In order to more effectively control continuous casting and various other thermomechanical processing treatments (for example, liquid center rolling), it is important to have accurate knowledge of both surface and internal temperature. The objective of this program is the development of a sensor for the rapid direct measurement of temperature distributions in both solid and solidifying metal bodies.

Presently, temperature is determined on the basis of surface temperatures measured with radiation pyrometers, internal temperatures selectively measured with thermocouples, or temperatures inferred from process parameters (for example, rolling pressure). Computer-based thermal models are also increasingly being used to predict temperature distributions but with only varying degrees of

success. Each has associated limitations and difficulties and alone are unable to satisfy present needs.

An ideal temperature sensor would measure temperature to within $\pm 10^{\circ}\text{C}$ with a spatial resolution of $< 5\text{ mm}$ over a temperature range of $500^{\circ} - 1350^{\circ}\text{C}$ without need to physically contact the body. It should be capable of giving a reading within a few seconds and be unaffected by the presence of combustion gas products or nearby heat sources.

There are numerous potential applications for a temperature sensor during steel processing. They include:

- Control of cooling during continuous casting.
- Reheat furnace control.
- Hot connection rolling of continuously cast slabs.
- Batch annealing furnace control.

During continuous casting, for example, it would be desirable to mount sensors just after the strand exits the mold, at several locations in the cooling region, and before the stand is cut into lengths. This would enable solid shell thickness to be continuously monitored, and allow calculation of the heat transferred through the mold and during various stages of spray cooling. In turn, this would enable faster casting speeds, and thus productivity improvements estimated to be $\sim 5\%$.

Calculations have shown that full implementation of such a sensor in 1982 would have resulted in \$275 million savings in energy and productivity improvements annually for the domestic steel industry.

The task force unit evaluated a variety of candidate measurement methodologies including ultrasonics, eddy currents, neutron thermalization and radiography. The ultrasonic approach was deemed in 1983 to have the greatest likelihood of success although the eddy current approach also had much to commend it. Discussions were held both with the National Bureau of Standards (NBS) and the Battelle Pacific Northwest Laboratory (PNL) that ultimately led to complimentary research programs at both laboratories. The program at PNL was co-funded by AISI and the U.S. Department of Energy. The program at NBS was arranged somewhat differently. NBS assigned its staff to the area while task force funds were used by the AISI to sponsor the reassignment of steel industry researchers to NBS to participate in the research program. The programs at both NBS and PNL also interacted with vendors of high temperature electromagnetic acoustic transducers (EMAT's).

The ultrasonic approach is based upon the strong dependence of ultrasonic velocity with temperature (Fig. 2). Each steel has a slightly different dependence, but for most, the velocity of longitudinal waves generally decreases with temperature at a rate of between 0.5 and $1.0 \text{ ms}^{-1} \text{ }^\circ\text{C}^{-1}$. Thus, if the internal velocity distribution within a hot steel body can be measured, then the temperature distribution can be inferred using calibration data such as that shown in Fig. 2. The problem of developing a temperature distribution sensor resolves itself into the separate problems of reconstructing an ultrasonic velocity profile (or distribution) within a body, obtaining reference data relating ultrasonic velocity to temperature and the development of ultrasonic instrumentation suitable for reliable high temperature work in a mill environment.

The latter aspect to the program is presently being addressed by the use of (remote) high intensity pulsed laser generation of ultrasound coupled with noncontact EMAT detection. This avoids the need to physically contact the steel. Such an approach has been demonstrated to be feasible in the laboratory on cooling steel bodies at temperatures up to $\sim 750^\circ\text{C}$ (Ref. 3). This upper temperature limitation results from the high temperature degradation of EMAT performance, a limitation that is being addressed in present work at PNL.

The reconstruction of a velocity distribution is being tackled by two approaches. One is an extension of time-of-flight (TOF) tomography, while the second is a novel approach that we refer to as dimensional resonance imaging. In the tomographic approach (Fig. 3), the time-of-flight of ultrasonic pulses along ray paths of known lengths are used to determine the coefficients of a series representation of the temperature field. To date, profiles have been determined for stainless blocks of both cylindrical and square cross section at temperatures up to 750°C (Fig. 4).

A potential concern with the TOF approach is high frequency ultrasonic scattering by large columnar grains in solidifying bodies and dissipation of high frequency signal components by temperature dependent internal friction mechanisms in solidified steel at high temperature. In anticipation of this, a new low frequency resonance method has also been developed and successfully used to reconstruct temperature profiles in model laboratory experiments. This approach is based upon the shifts in dimensional resonance frequencies from integer multiple values of the fundamental when a distribution of modulus/density exists within. An example reconstruction is shown in Fig. 5, where a 1.6°C temperature change was resolved in a 36" long aluminum bar. Because the frequencies of interest are very low (in the kHz range), grain scattering and internal friction losses are minimized, and sensitive temperature measurements are attainable.

The present objectives are to develop a complete prototype sensor specification during 1986 and to construct and evaluate the sensor at selective mill sites during 1987.

AUTOMATIC DETECTION OF PIPE AND GROSS POROSITY IN HOT STEEL BILLETS, BLOOMS OR SLABS

The objective of this sensor development program, more than any other, is changing with time due to a fundamental shift in solidification practice within the steel industry. At the outset of the program, the majority of steel was solidified by ingot casting methods and thus pipe and gross porosity were important quantities to locate for control of ingot cropping. With the move to continuous casting, interest is shifting to the development of a sensor to locate small scale porosity and detect segregates, defects that are the cause of poor quality during continuous casting. This has resulted in a continuous need for spatial resolution improvement in the sensor.

The initial aim of the program was development of a sensor to detect primary pipe and gross porosity in hot, primary-rolled materials in order to provide sufficient information to determine an optimum cropping point. The sensor was expected to:

- Locate the edge of pipe to within 1/10" slabs up to 12 inches thick.
- Detect and locate pores greater than 1/3" in diameter.
- Perform a two dimension scan within 30 s or less.
- Be capable of operation at steel surface temperatures of 830°-1100°F.

The availability of such a sensor would benefit productivity and yield through the avoidance of discarding sound steel. In 1982, yield improvements of as little as 0.5% were considered capable of generating a \$50 million benefit to the domestic industry annually. Other benefits would accrue from an improved quality through avoidance of pipe and porosity in finished material. This would help counter foreign competition, lead to greater customer satisfaction, and result in significant energy savings by eliminating the need to cool to ambient temperature to perform internal (ultrasonic) inspections.

Past research had shown ultrasonic scattering to be capable of detecting defects of the size of interest when the steel was at ambient temperature (where it is simple to get good ultrasonic coupling). On hot products, however, it is necessary to thermally protect the sensitive piezoelectric materials used to generate and detect ultrasound. This has been achieved in the past through the use of cooled metal bars (buffer rods). One (cooled) end is attached to a piezoelectric transducer, and the other pressed against the body to be inspected (Fig. 6). While the approach was sufficiently sensitive, very large pressures were found necessary in order to couple the ultrasound into the steel body (Ref. 4). This was found to cause the system to be mechanically unreliable and very slow. The adoption of noncontact ultrasonic approaches similar to those proposed for a temperature sensor therefore appears to

be a promising route to a solution, though one not expected to be realizable in the short term, given the still developing state of noncontact ultrasound technology.

The pressing need for a short term, at least partial solution, to the problem resulted in the evolution of a dual-thrust collaborative program involving the AISI, Magnasonics*, Magnaflux*, NBS and more recently the Argonne National Laboratory (ANL). The short term (interim) solution was to be addressed by evaluation of a rolling wheel contact method proposed by the Magnaflux Corporation. The approach featured a rolling wheel (in place of a buffer rod) that promised to overcome the scan speed limitation. The longer term solution was perceived to be the development of high temperature EMAT's and (possibly) pulsed laser excitation of ultrasound. From a technical viewpoint, the early implementation of a contact method was also perceived to be a useful means for gathering important information about the ultrasonic scattering properties of realistic defects and the nature of wave propagation in very hot (as-cast microstructure) steels. Thus information would be important in guiding the longer term noncontact approach.

Research to date has shown the contact wheel approach to be capable of the required resolution and speed at ambient temperature where vacuum grease couplants can be used to eliminate the need for high pressure. However, at higher temperatures, these particular couplants do not work, and high pressure and alternative couplants based upon various salts, glasses and fluxes have been investigated in research at NBS and Magnaflux. One couplant in particular, borax, has been found by NBS to give excellent ultrasonic coupling, even at 1100-1200°C. For example, in Fig. 7, we show the signal from a pitch-catch ultrasonic configuration, (shown in Fig. 6) in one case at ambient temperature using a vacuum grease couplant, and in the other at 800°C using borax. Given that ultrasonic propagation is usually worse in steel at high temperature, the better signal-to-noise ratio of the defects signifies a very high coupling efficiency, sufficient to eliminate all need for additional pressure coupling.

Prior to installing a prototype rolling wheel system in a mill, full scale trials are being conducted at the ANL where heating/handling facilities exist for large steel bodies. Encouraging progress has been made to date, and plans are progressing for mill evaluation of a prototype within one year.

Encouraging progress has also been made with the noncontact approach. Electromagnetic acoustic transducers have been designed for both ultrasound generation and detection with optimum sensitivity for the pipe/porosity detection at high temperatures. They have been evaluated at temperature on ferritic steels both above and below the Curie temperature. As noncontact generators of ultrasound, EMAT's to date are not as efficient as would be desired, but improvements are being pursued. As receivers of laser excited ultrasonic pulses, considerable early success has been achieved, encouraging us to believe that a noncontact solution may be viable within a few years. Work is also continuing to

optimize the instrumentation, improve its survivability at high temperature, develop signal processing software and to improve spatial resolution for the detection of small defects.

THE FUTURE

The collaborative research programs initiated by the AISI are each now showing promise of at least partially solving the most immediate sensor needs of the steel industry. As encouraging as this research progress is, the ultimate test of its usefulness will be the industry implementation of these process control tools. This may be as difficult to achieve as the research has been to perform because it raises several, as yet unresolved, issues. For instance who will build and install these sophisticated sensors in steel mills? Surely this is not a task suitable for the federal laboratories involved in much of the research nor the steel companies themselves, who no longer retain the necessary in-house expertise. The most promising approach at this time appears to be the assignment of the technology to vendor companies under some form of license arrangement that protects the vendors subsequent investment. The emergence of an economically healthy, state-of-the-art sensor vendor industry therefore seems to be an important factor in determining the future availability of process control sensors for steel. The industry must therefore now look to ways to promote this important development.

The collaborative nature of the research programs described above arose because of a shared need for sensors by the entire domestic steel industry, combined with their high development cost and risk (prohibitively high for a single company). These factors are seen increasingly in other steel research areas, for example, in the development of new processing technologies such as thin strip casting. Here also strong collaborative programs are now emerging with the intent of advancing the competitiveness of the domestic industry in the international marketplace. It seems that collaborative efforts are on the increase, and those for sensors can form a model for this approach to meeting the research needs of an industry. The careful ways in which research needs were identified, ongoing research monitored, and results disseminated provide good guidelines for all collaborative programs. The reassignment of steel industry staff to the laboratories pursuing research has been a particularly effective two-way technology transfer mechanism.

At the beginning of the programs, sensors, were viewed as inprocess inspection tools or as useful adjuncts to existing process control strategies. However, recently, the very exciting opportunity of a new process control strategy, the so-called Intelligent Processing of Materials, is now beginning to emerge hand-in-hand with the emergence of these sensors (Ref. 5). Intelligent process control involves three elements:

- Predictive process models.
- Sensors.
- Control systems featuring artificial intelligence/expert systems.

For example, sophisticated models for alloy solidification have been developed in recent years and are presently used to define operational conditions during continuous casting. These models need, as inputs, information about key process and microstructure variables (temperature gradient, solidification interface velocity, interface morphology, heat transfer rates, etc.). Presently estimated values are used and this introduces substantial uncertainties. The development of sensors able to measure these quantities in process greatly expands the usefulness of the process models, for now they can make detailed accurate predictions of the current state of solidification. Adjusting control parameters (such as heat extraction rate, mold lubricity, casting rate, etc.) then provides a means for continuously maintaining optimal solidification conditions consistent with productivity requirements. However, with numerous (nonlinear) interacting variables to be controlled in rapid time frames, automated control schemes are required. It is the recent development of artificial intelligence/expert systems that offers such great promise for such control schemes.

Intelligent processing of materials is consistent with the implementation of full factory automation systems and with them, the opportunity to attain substantial productivity and quality improvements. The development of intelligent processing strategies may also expose opportunities to implement commercially entirely new methods of processing -- methods hitherto considered too unstable for commercial utilization -- a development that would truly advance the competitiveness of domestic materials producing industries.

ACKNOWLEDGEMENTS

In preparing this report, I have drawn heavily upon unpublished research prospectuses developed by AISI Task Force Units. I am also grateful to the AISI for permission for this. I am grateful to Drs. Y. Kim, T. Porter, F. Achey, D. Rogers, J. Cook, W. Wilson, B. Sylvester, K. Kappmeyer, R.D. Jeffress and W. E. Dennis who have provided most helpful discussions on numerous aspects of the work reported.

Disclaimer: Individual companies are mentioned in this paper for the purpose of accurately representing the research groups involved in collaborative programs. This should not be construed as an NBS endorsement of their products.

REFERENCES

1. Steel Industry Research Priorities for Process Control and Sensor Development. 1981, AISI Internal Report.
2. R. Mehrabian, R.L. Whiteley, E.C. van Reuth and H.N.G. Wadley, 1982, Process Control Sensors for the Steel Industry: Workshop Report, National Bureau of Standards Internal Report 82-2618.
3. H.N.G. Wadley, S.J. Norton, F. Mauer and B. Droney, Ultrasonic Measurement of Internal Temperature Distribution, Proc. Roy. Soc. (London), 1986, In Press.
4. B.E. Droney and T. J. Pfeiffer, Ultrasonic Inspection of Hot Steel Blooms to detect Internal Pipe, Mat. Eval. June 1980, p. 31.
5. R. Mehrabian and H.N.G. Wadley, Needs for Process Control in Advanced Processing of Materials, Journal of Metals, Feb.1985, p. 51.

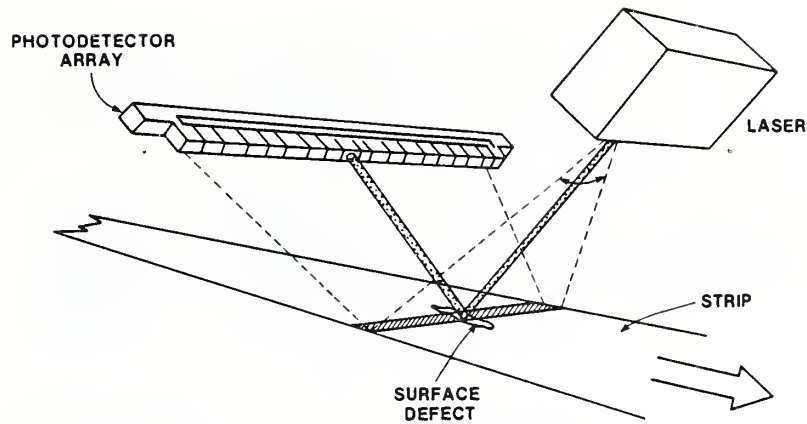


Fig. 1 A photodiode array is used to detect the coherent light scattered by defects on moving metal strip.

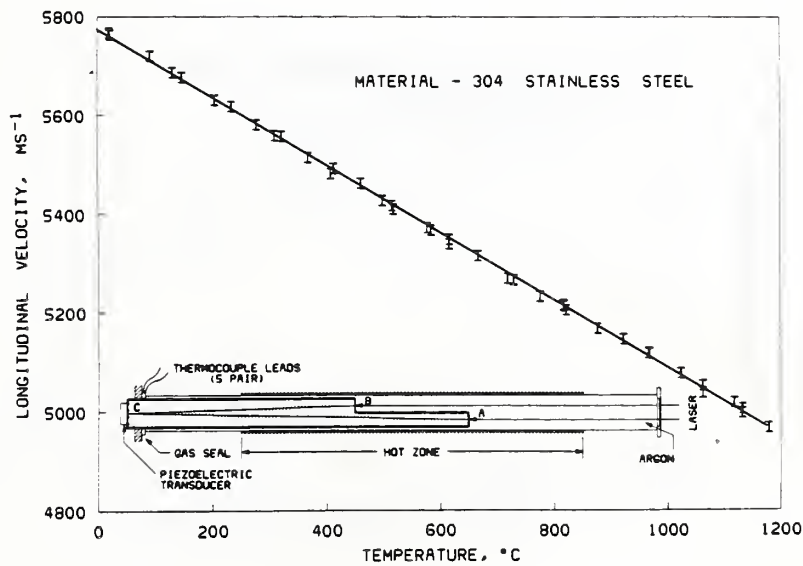


Fig. 2 The dependence of ultrasonic velocity upon temperature for AISI 304 stainless steel. The insert shows the experimental configuration used to measure ultrasonic time-of-flight between points A and B.

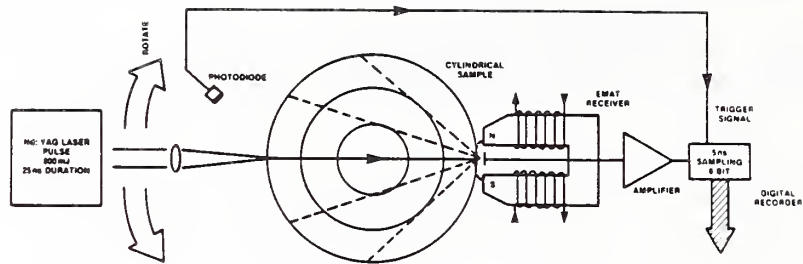


Fig. 3 An intense laser pulse is used to induce a strong ultrasonic pulse whose time-of-flight over various ray paths is measured using an EMAT and associated high speed digital instrumentation.

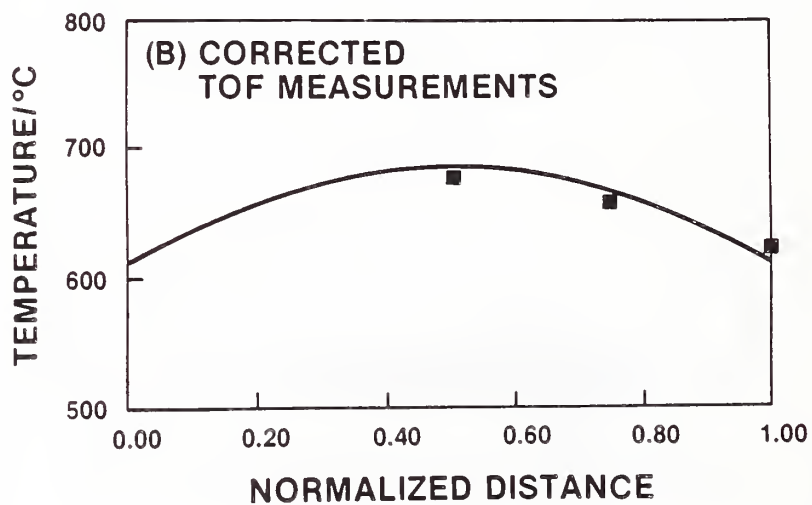


Fig. 4. A reconstructed temperature profile through the thickness of a six inch thick 304 stainless steel block (curve). Also shown are simultaneously recorded thermocouple measured temperatures for comparison.

Measurement of Internal Temperature Distribution

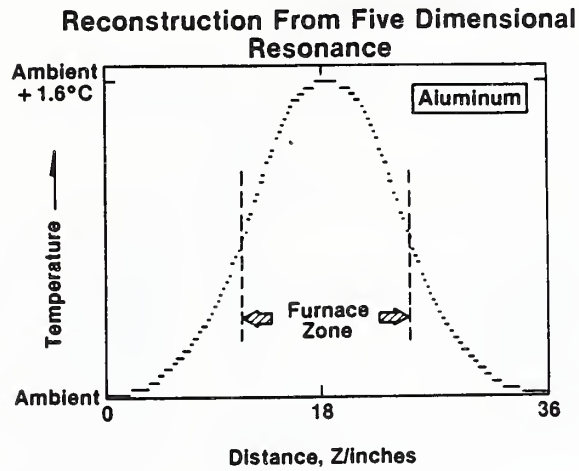


Fig. 5. A reconstructed temperature profile using the dimensional resonance technique.

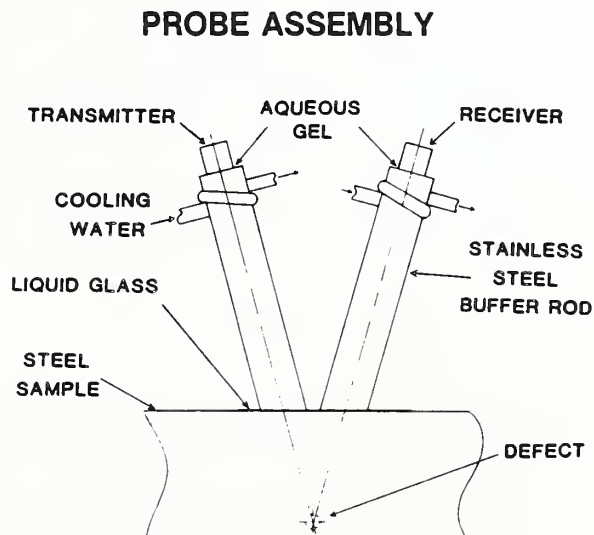


Fig. 6. Cooled steel bars can be used to thermally isolate ultrasonic transducers.

FLAW SIGNALS

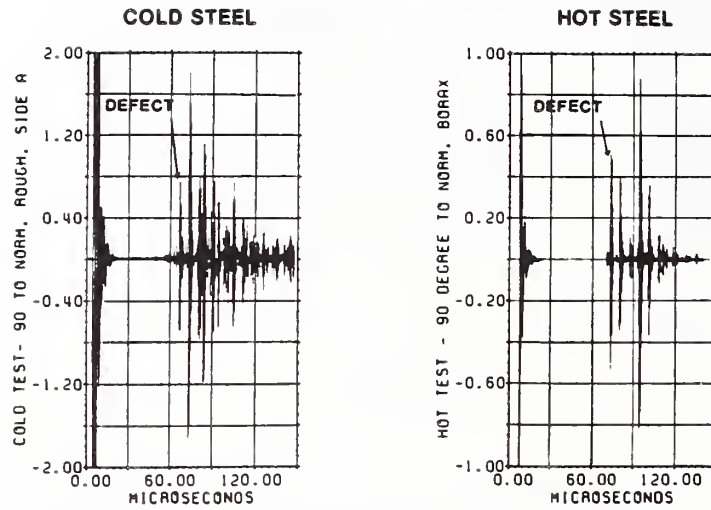


Fig. 7. Ultrasonic waveforms showing detection of defect echos at ambient and 800°C.

RECENT PROGRESS IN THE EVALUATION OF A PIPE/POROSITY SENSOR

DAVID KUPPERMAN

Argonne National Laboratory
Argonne, IL 60439

INTRODUCTION

In primary rolled ingot steel, a variety of both large and small imperfections occur at the end of the rolled slab, and must be sheared off prior to conversion into a final product. Presently, visual observations on steel at 2000°F are used to estimate the optimum amount of material removed by cropping. These observations are insufficient to determine the point within the steel where flaws end and "sound" steel begins. Thus, overconservative cropping is often practiced that leads to \$50 million losses in the domestic industry annually.

To help alleviate this problem, a new device, that can detect imperfections as small as 0.25" within hot steel slabs, has been developed during a two-year collaborative effort between AISI member companies, NBS, and Magnaflux Corporation. The new development, a "high-temperature imperfection detector" uses ultrasonic pulses to detect internal discontinuities in hot steel. In operation, a transducer capable of generating ultrasonic pulses, is in contact with the inside rim of a three-foot diameter stainless steel wheel (Fig. 1). This wheel rotates as steel slabs at 2000°F pass underneath. The transmitted ultrasonic pulses transmitted into the steel through the rim are reflected by internal discontinuities. These reflected signals pass back into the wheel and are detected by a receiver transducer. To evaluate the device, a hot testing facility has been assembled at the Argonne National Laboratory (ANL) and tests conducted upon numerous samples containing naturally occurring defects representative of those encountered in a primary rolling mill.

PROTOTYPE EVALUATION

The prototype device described above is augmented by a computer based analysis system that records the amplitude and time-of-flight of reflected pulses. The system then produces a color map of the internal defect structure. Each imperfection is outlined according to size and location and is color coded based upon the amplitude of the detected ultrasonic reflection.

The ultrasonic system has been designed to scan representative 8" x 18" x 20" slab sections that are near the cropping temperature of 2000°F. The configuration and slower speed of this prototype depart somewhat from that



Fig. 1 A photograph of the contact ultrasonic sensor undergoing evaluation upon a hot steel billet at the Argonne National Laboratory.

which eventually will be required for production installations; however, the use of multiple transducers and a faster computer will overcome these problems.

For the thick steel slabs evaluated, a one-sided "pitch-catch" split wheel was selected. However, the system configuration, size, and approach could be conveniently changed for billet, bar, tube, and strip applications (Fig. 2).

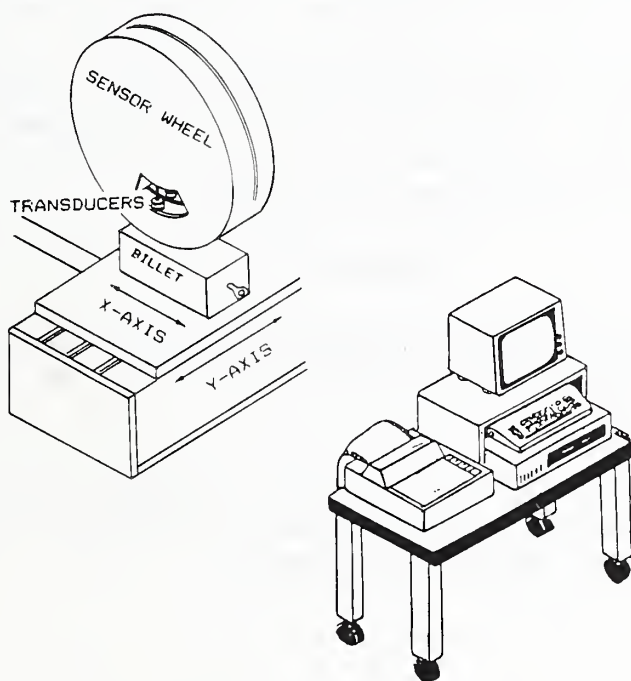


Fig. 2 The split wheel ultrasonic sensor developed for detection of gross porosity and pipe.

Ultrasonic coupling is a major problem. Work carried out at Argonne led to the following conclusions; either of the following three methods could be applied for coupling of the ultrasonic waves to the hot steel: (a) high pressure direct coupling; (b) magnesium oxide powder with moderate pressure; or (c) melted borax with very minimal pressure. To ensure long-term system mechanical reliability, the melted borax approach may be preferred. In the event the borax is applied, a zirconium or other protective coating would be applied to sections of the stainless steel wheel to avoid the corrosive effects of borax.

Several comparison between cold ultrasonic immersion tank images and the color images from hot testing provided progressively improved correlation as the testing's program was carried out. Eight-inch crop ends, containing primary pipe, fishtail, and secondary pipe, were scanned with the wheel in both cold and hot states. In addition, system repeatability was checked and correlation was excellent. The adequacy of the thermal analysis was also demonstrated by successfully predicting resulting temperature changes in the wheel and ultrasonic probe.

The most recent tests of the sensor system at Argonne (including a successful demonstration to representatives of 24 steel companies) have confirmed that such a device could be used inline within a steel mill environment to clearly define the imperfections in hot steel. A defect as small as 1/4" in diameter can be detected at 2000°F (Ref. 2). The widespread use of this concept in steel rolling and continuous castings could result in considerable monetary savings that would improve the American steel industry competitiveness throughout the world.

REFERENCES

1. C.D. Rogers, B.E. Droney, J.M. Toth and H.N.G. Wadley "Detection of Pipe and Porosity in Hot Steel Slabs, Blooms and Billets", Proc. 26th Mechanical Working and Steel Processing Conference, October 1984.
2. D. Kupperman, "Design and Testing of a Prototype Contact Ultrasonic Sensor System for Detecting Gross Porosity within Thick Hot Steel Slabs, Blooms and Billets", In preparation.

A PULSED LASER/ELECTROMAGNETIC ACOUSTIC TRANSDUCER APPROACH TO ULTRASONIC SENSOR NEEDS FOR STEEL PROCESSING

G.A. ALERS

Magnasonics, Inc.
215 Sierra Drive, SE
Albuquerque, NM 87108

INTRODUCTION

Many of the traditional NDE techniques of the past are today being investigated for their potential role as process control sensors for materials processing (Ref. 1). Ultrasonic inspection appears one of the most promising because of its ability to penetrate opaque bodies and to allow determination of microstructure variables (such as grain size), process variables (such as internal temperature distribution) and detect internal discontinuities (cracks, pores and inclusions). A key problem with the traditional approaches to ultrasonic measurements is the need to contact the body being probed with piezoelectric transducers. These transducers are fragile, require couplants, and fail when exposed to temperatures of more than a few hundred °C. Their use during processing may thus require practices that unacceptably interfere with the process.

Pulsed lasers for remote ultrasonic generation have been available for several years. Their use would overcome all the difficulties above if a similar remote ultrasonic receiver were available. The obvious candidate for this would be a laser interferometer, but it is of insufficient sensitivity for applications which involve unpolished, poorly reflecting surfaces. An alternative noncontact (but no longer remote) receiver could be an electromagnetic acoustic transducer (EMAT). This has the potential to be engineered to survive the process environment, and if carefully designed, to match the characteristics of a laser ultrasonic source.

Electromagnetic Acoustic Transducers (EMATs) are noncontact ultrasonic transducers that can operate on metals across a small air gap. Thus, they should be applicable to the problem of defect detection in steel at very high temperatures. During the past few years, the AISI and NBS have sponsored an advanced development program aimed at demonstrating the proof-of-principle for combining an EMAT ultrasonic receiver with a pulsed laser generator of ultrasonic pulses. This report summarizes the results obtained to date and includes an addendum describing very recent developments sponsored by the DOE and Battelle Northwest Laboratories.

LASER GENERATED ULTRASOUND

The generation and subsequent propagation of ultrasound by the absorption of an intense laser pulse is now a relatively well understood process (Ref. 2). Research at Hull University and Harwell in England during the early 1980's indicated that two modes of laser generated ultrasound may occur. For low absorbed fluxes, the surface where absorption occurs never exceeds its melting temperature and the source of ultrasound is then a transient dilatation. The stresses associated with this dilatation are for the most part below the elastic limit, and this mode of generation is therefore referred to as thermoelastic. At higher fluxes, the surface temperature rise is capable of exceeding the vaporization temperature. Atoms leave the surface at high velocity imparting a momentum to the substrate that is the source of ultrasound. This mode of generation is referred to as ablation.

It is possible to model the thermoeleastic source using heat flow theory. For simple bodies, such as isotropic elastic half-spaces and infinite plates, this theoretical description of the source can be coupled with the bodies dynamic elastic Green's tensor of the bodies to quantitatively predict the temporal waveform of the ultrasonic signal (Ref. 2-4). The displacement signals at epicenter and various locations on the plate surface are shown in Ref. 3. The response of an EMAT is proportional to surface velocity and so the velocity at the longitudinal arrival at epicenter is a positive pulse whose half width is approximately that of the source duration (in the absence of grain/scattering absorption) while at the shear arrival it is a negative pulse.

The ablative source is not so amenable to quantitative modelling because we do not know the mass or velocity of material ablated, or how this varies with time during optical absorption. However, if it is assumed that the source is mechanically equivalent to a momentum of arbitrary strength, temporal waveforms of arbitrary amplitude may then readily be evaluated (Ref. 2). As seen by an EMAT, the principle difference from a thermoelastic source is that the epicenter longitudinal arrival is now a bipolar pulse with an initially negative direction. For this source, the epicenter shear arrival remains a unipolar pulse but of opposite sign to that of the thermoelastic source.

In practice, it is not possible to produce pure ablation without accompanying thermoelastic contributions to the source. The relative contributions of each to the emitted ultrasound are yet to be fully resolved, and will vary with optical flux. However, the interesting possibility exists of identifying a range where only longitudinal waves propagate because of cancellation of the shear components due to thermoelastic and ablative sources.

The displacement amplitude of a laser generated ultrasonic signal is proportional to the absorbed optical energy in the thermoelastic region. Thus, the velocity amplitude will be proportional to the absorbed optical power. This should be maximized if we wish to maximize the EMAT signal:noise ratio. At NBS, a Q-switched Nd:YAG laser is available with a 25 ns pulse duration and variable energy per pulse up to 800 mJ (average power of 32 MW). 175 mJ, 1 mm diameter pulses were used for the results reported here.

EMAT ULTRASONIC RECEIVERS

Although the EMAT is technically a noncontact ultrasonic transducer, it must be held close to the surface before the electromagnetic induction process can operate with a useful efficiency. For application to inspection of hot steel, any small air gap at the surface of the metal acts as a good thermal insulator and greatly reduces the heat transfer into the transducer structure. In addition to being physically capable of operating in a high temperature environment, the EMAT has several other features that can be exploited to advantage. By simply changing the direction of the magnetic field used, the transducer can be made to detect either longitudinal or shear waves. Also, by choosing the shape of the coil of wire inside the EMAT, the angle of incidence of the waves to which it is sensitive can be controlled. Since the electromagnetic induction process can be made to operate over a wide range of frequencies, EMATs are fundamentally broadband devices. Their frequency of operation is usually set by the electronic receiver circuits used to amplify the electrical signals. For hot steel, the best frequency of operation is determined primarily by the laser source spectrum, the ultrasonic attenuation properties of the steel and only secondarily by the structure of the EMAT and its associated electronic circuits.

An important problem to be overcome when designing an EMAT for operation on hot steel is to be sure that the electrical resistivity of the hot steel is not so high that the electromagnetic skin depth becomes comparable with the wavelength of the ultrasonic waves involved. For ordinary metals with resistivities near 10 $\mu\text{ohm-cm}$, this criterion is easily satisfied for frequencies less than 10 MHz. However, hot steel has a resistivity between 100 and 200 $\mu\text{ohm-cm}$ so the frequency response may be attenuated above 1 MHz for longitudinal waves and 0.3 MHz for shear waves.

EMAT DESIGN

Since an EMAT consists of a coil of wire held close to the surface of the part being inspected plus a large magnetic field to flood the region around the coil, two problems must be addressed to enable hot steel bodies to be interrogated. First, the coil must be constructed with high melting point wires and a layer of thermal insulation between the coil and the steel. Second, the

magnet must be designed to supply a large magnetic field to the total area of the EMAT coil and must be protected from the heat generated by the hot steel.

The most direct approach to supplying a magnetic field to the EMAT coil is to use a large electromagnet with pole pieces designed to concentrate the magnetic flux at the EMAT coils, as shown in Fig. 1(a). Here, the EMAT coils can be located in either a normal or tangential field direction and hence to receive either longitudinal or shear waves. (Position A in a tangential field is suitable for longitudinal waves while position B, in a normal field, is suitable for shear waves.) Such an electromagnet was constructed but proved to be quite massive and difficult to move in a scanning apparatus even though it generated magnetic fields in the 4 to 5 koe range at an EMAT coil with a 1/2" diameter. Figures 1(b) and (c) show magnet configurations based on samarium cobalt permanent magnets located very close to the EMAT coil itself in order to maximize the fields at the coil wires. Both of these structures were assembled out of 1/4" thick by 1/2" square slabs of SmCo and fields in the range of 3 to 4 koe were measured at the EMAT coil positions. These permanent magnet structures were quite light and maneuverable and thus could be easily scanned over large areas. Their reduction in efficiency caused by slightly smaller magnetic fields could be tolerated in exchange for this simplification in mechanical structure.

The EMAT coils were made thermally stable by housing their copper wires in small (1/16" diameter), four-hole ceramic thermocouple tubes. Since the duration of the exposure to high temperature was intended to be short in order to protect the permanent magnets, it was deemed unnecessary to use more expensive, high resistance wires such as platinum for the EMAT coils. By using thermocouples tubes with 1/16" diameters, the minimum liftoff or separation between the EMAT coil and the sample was 1/32" (0.8 mm). In the regions at the ends of the thermocouple tubes where the copper wires were unprotected, the wires were coated with a high temperature ceramic cement that served to thermally and electrically insulate each wire from its surroundings.

Since it was of interest to make time-of-flight measurements and since the attenuation of high frequency shear waves in hot steel is higher than longitudinal waves (Ref. 5), the high temperature EMAT designed to detect longitudinal waves propagating directly through the thickness dimension of the steel samples received the most attention. Thus, the comb magnet construction technique shown in Fig. 1(c) was used in all the experiments reported here. All the wires in each section of the EMAT coil between the pole pieces conducted current in the same direction but this direction reversed in the adjacent pole piece gap where the magnetic field was also in the opposite direction. In this way, the entire face of the EMAT would respond in phase to a plane longitudinal wave striking the face along its

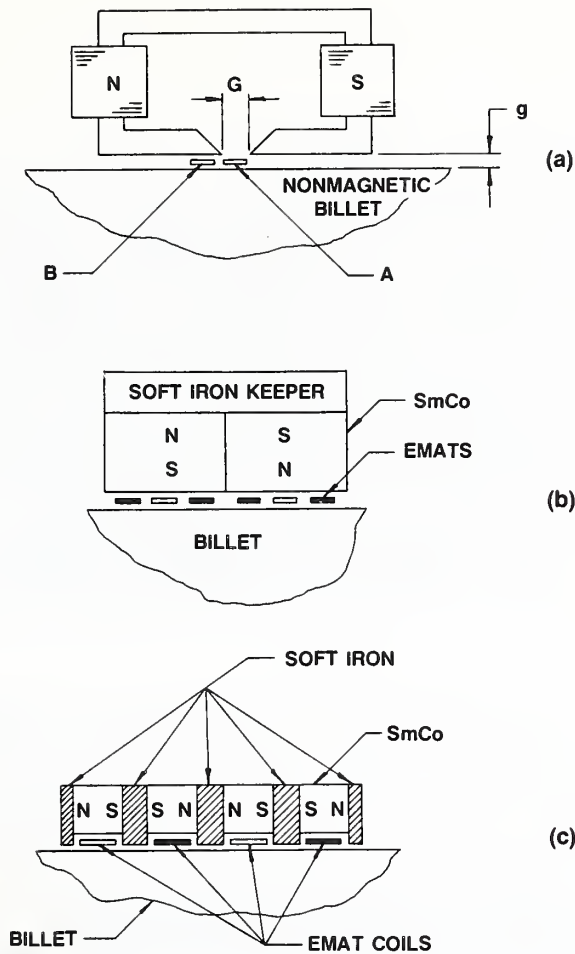


Fig. 1 Magnet configuration needed to operate EMATs. (a) Electromagnet for exciting or detecting either longitudinal or shear waves. (b) Permanent magnet arrangement for exciting or detecting shear waves. (c) Permanent magnet design for excitation or detection of longitudinal waves.

normal direction. This method of assembling the permanent magnet structure allows the pole pieces to conduct heat directly to the samarium cobalt. Thus, the ability of the probe to operate on hot objects depended critically on the length of time it took to heat the permanent magnets to a temperature at which their performance was jeopardized. The manufacturer of the magnets used in these EMATs set the upper temperature limit for his product at 330°C for continuous operation. During the tests on hot steel blocks, a thermocouple on the samarium cobalt showed that it required over 1-1/2 minutes for the temperature of the magnets to exceed 250°C. This 90 s interval was ample time for collecting all the necessary ultrasonic information. Therefore, it was not necessary to add cumbersome water cooling apparatus at this stage.

RESULTS

In accord with the ablative mechanism of generating ultrasonic waves, very large ultrasonic signals were observed with the longitudinal wave EMAT shown in Fig. 1(c) when it was positioned on the face of a sample directly opposite to the point at which the laser beam struck the sample. When a shear wave sensitive EMAT was used (Fig. 1(b)), shear waves were detected only when the EMAT was displaced from epicenter along the back side of the sample. As expected from EMAT theory (Ref. 6), shear waves at an angle of 30° relative to the surface normal were easily detected. One surprising result was the observation of a second large shear wave signal leaving the surface of optical impact at an angle of 60° relative to the surface normal. This may be a manifestation of the thermoelastic contribution to the source.

A very important performance characteristic of the longitudinal wave EMAT used here was the amount of air gap or liftoff that could be tolerated between the sample and the front face of the EMAT. Figure 2 shows how the output signal from the EMAT decreased as a function of this separation distance. This graph shows that the addition of up to 0.02" of thermally insulating material between the pole pieces and the hot object would not cause a significant reduction in sensitivity but would probably make a dramatic improvement in the ability of the structure to withstand exposure to high temperatures. The fact that the drop in signal strength is described by an exponential function is consistent with the periodic structure of this form of magnet. The rate of drop could be decreased (to achieve higher sensitivity at large air gaps) by using thicker permanent magnets to increase the separation distance between pole pieces.

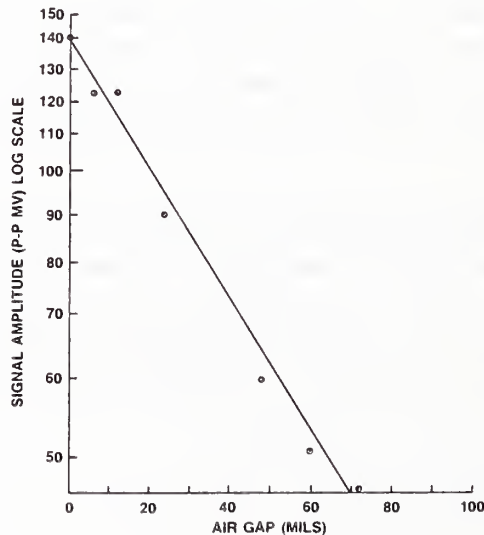


Fig. 2 Dependence of the EMAT receiver probe sensitivity on the thickness of the air gap between the probe and the surface of the sample.

A second important performance characteristic of the longitudinal wave EMAT used here was the frequency bandwidth that could be achieved with that specific EMAT design and amplifier circuit. Figure 3 shows the waveforms observed when the longitudinal wave EMAT shown in Fig. 1(c) was used to receive directly transmitted longitudinal waves generated by the pulsed laser. When narrow band filters were used in the amplifier stages, the waveform shown in Fig. 3(a) was observed. Note that the noise received prior to the ultrasonic wave arrival is very small and the electrical signal is a tone burst containing many cycles of oscillation. Figure 3(b) shows the effect of removing all the filters and tuning capacitors from across the EMAT coils to achieve a large bandwidth. The noise level prior to the arrival of the acoustic wave is much higher than in the previous cases. However, it appears that the arrival time could be measured to an accuracy greater than $0.1 \mu\text{s}$ (or 0.6%).

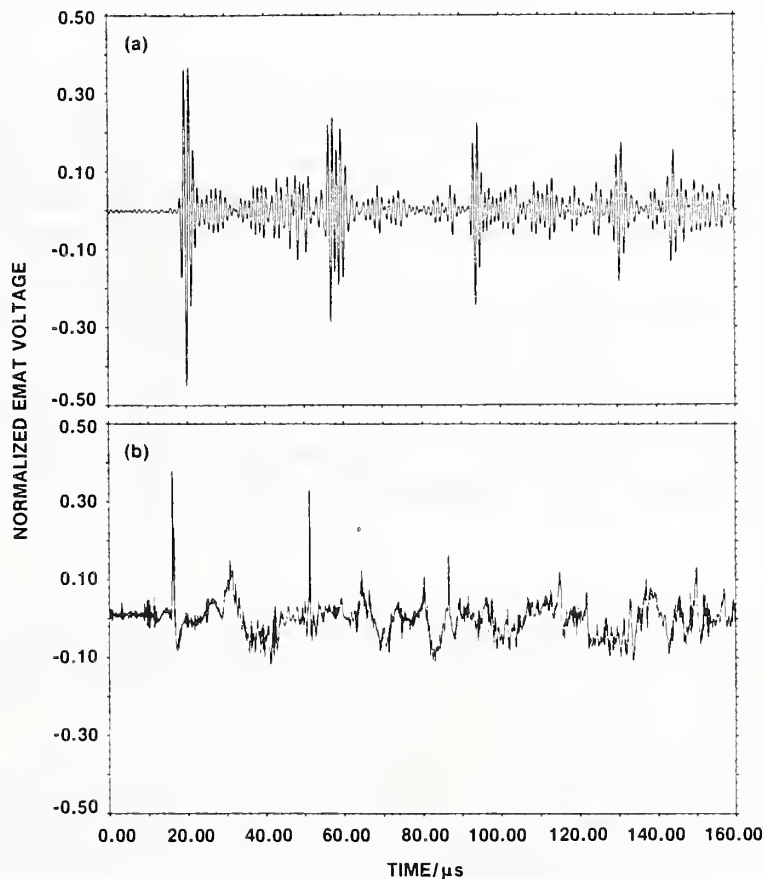


Fig. 3 Ultrasonic longitudinal waveforms observed with different electronic tuning circuits connected to the EMAT coil. (a) Band pass filter combined with a tuning capacitor across the EMAT coil. (b) No tuning.

In order to demonstrate laser excitation and EMAT reception of ultrasonic waves in hot steel, two large steel block samples were heated in a large furnace at 980°C (1800°F). One sample was made of 304 stainless steel and hence underwent no ferromagnetic transition as it cooled off. This sample was a 4" diameter cylinder in which the sound wave propagated along the 4" long axis of the cylinder. The second sample was a 6" by 6" square slab of 1018 steel arranged so that the sound wave propagated parallel to the 4" thickness dimension. For this sample, a transition from the nonmagnetic to magnetic state would be expected when the temperature passed through the Curie temperature of 770°C (1418°F). These hot blocks were positioned such that the focal point of the laser beam was at the center of the front surface of the sample. The EMAT was then rested lightly against the back surface directly opposite the laser impact point. Thermocouples were held against the sample surface and inserted into the EMAT structure at the location of the samarium cobalt permanent magnets in order to monitor the local temperatures while the steel cooled and the EMAT heated up.

Figure 4 shows examples of the waveform observed on the 4" long, stainless steel cylinder as its surface temperature fell from 752°C to 322°C. The directly transmitted longitudinal wave signal and three reverberations can be easily distinguished from the background noise. Most of this noise is probably from ultrasonic signals reflected by the side walls because the noise is at the EMAT frequency and increases with time after the laser impact. Note that the noise on the time interval immediately following the laser pulse and prior to the arrival of the first, longitudinal wave, signal is very low at all temperatures. As the sample became more cool, the acoustic noise between the reverberation signals increased. This may be explained by mode conversion at the side walls plus a dramatic lowering of the attenuation for shear waves formed by mode conversion as the temperature of the steel became lower.

Figure 5 shows the waveforms observed on the 4" thick slab of 1018 steel as the surface temperature dropped from 810°C (1490°F) through the Curie temperature to 618°C (1144°F). At the highest temperature studied, the ultrasonic longitudinal wave signals were very well defined and appear similar to the signals observed on stainless steel. Below the Curie temperature, the magnetic field from the pole pieces of the comb-type EMAT flowed directly into the steel in the immediate vicinity of the pole piece so that the tangential field at the EMAT coil became greatly reduced. Therefore, the sensitivity to longitudinal waves fell and the directly transmitted longitudinal wave which should arrive at about 20 μ s was no longer the dominant signal observed. Instead, a late arriving pair of signals appear, which are probably shear waves that have reached the EMAT by reflecting from the side walls of the sample. Since these shear waves have reflected

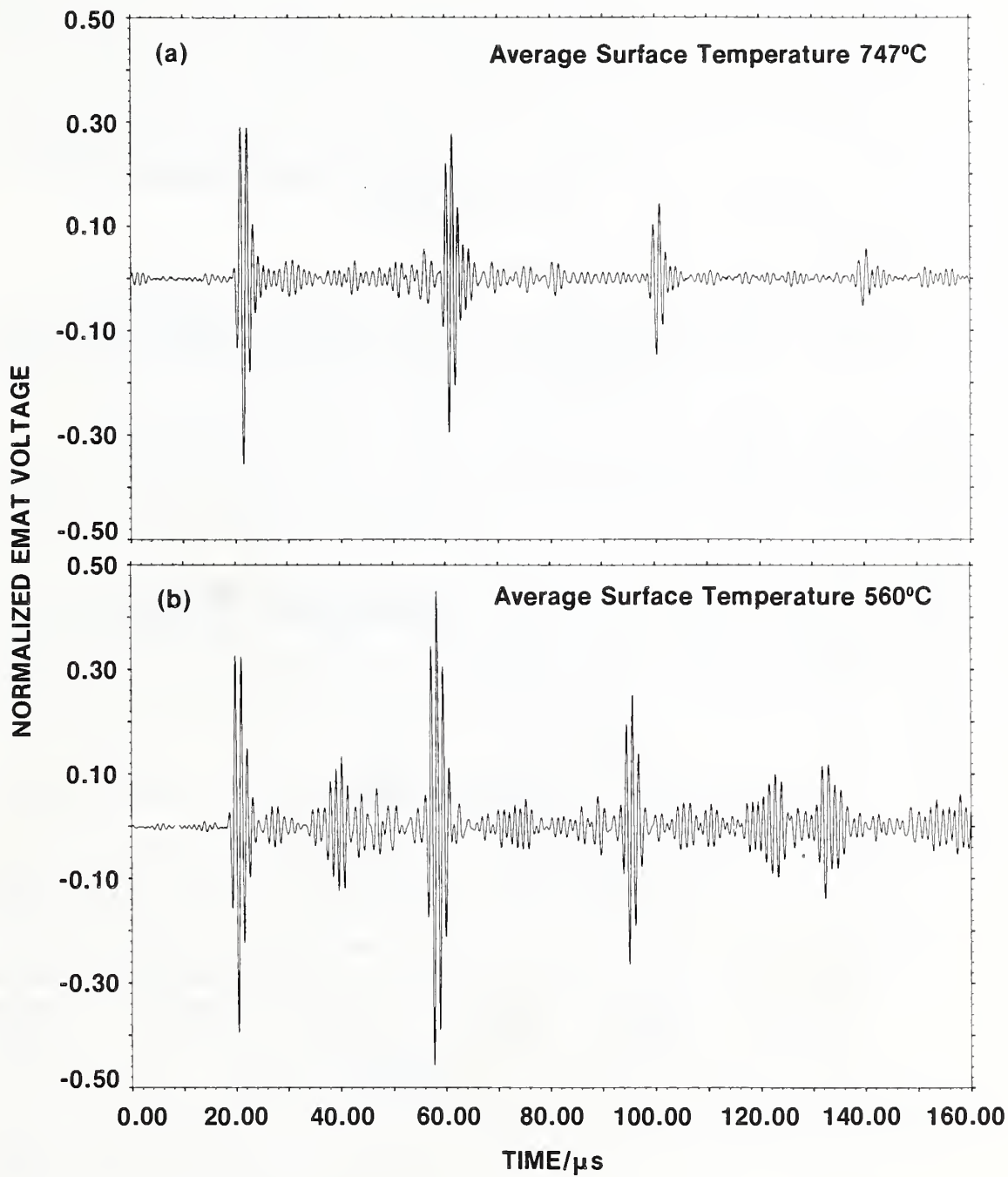


Fig. 4 Waveforms on a 4" thick stainless steel block.

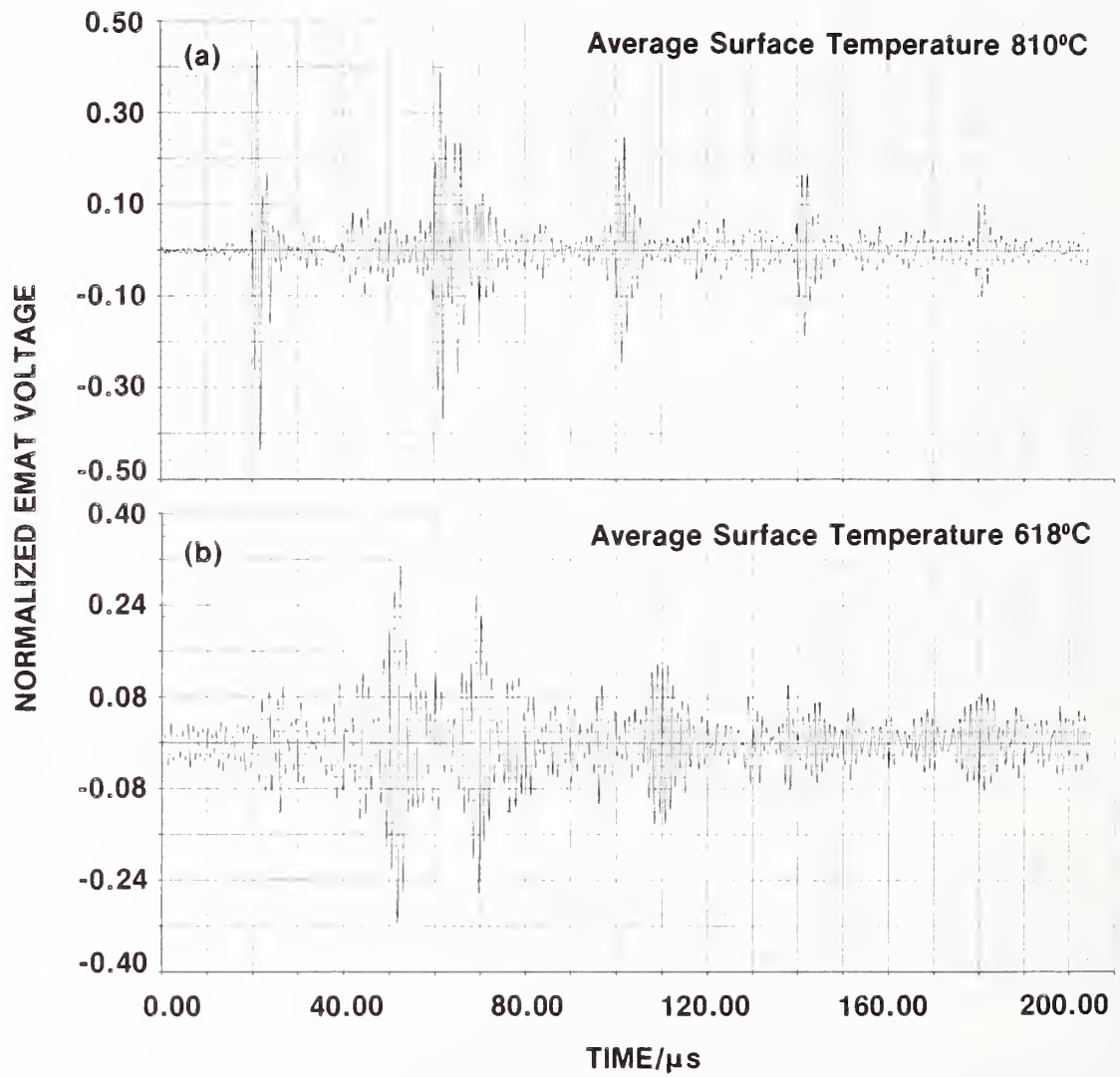


Fig. 5 Waveforms on a 4" thick 1018 block.

from the side of the sample, they must impinge on the EMAT at an angle and would be detected if a periodic normal magnetic field existed in the EMAT structure. Such a field is actually present in the immediate vicinity of the pole pieces of the comb-type EMAT when it is in contact with a sample that is ferromagnetic. An analysis of the geometrical dimensions of the EMAT used in these experiments indicates that the EMAT would be sensitive to shear waves that approach the face of the probe at an angle of about 48° relative to the surface normal. Such an angle is reasonably consistent with the sound wave paths reflected by the side walls of the sample.

CONCLUSIONS

1. A lightweight, easily scanned EMAT receiver probe has been constructed out of heat resistant materials and samarium cobalt permanent magnets to withstand intermittent use at high temperatures. It has been optimized for use with a pulsed laser ultrasonic source.
2. This probe was able to detect 1 MHz ultrasonic pulses generated by a focused 175 mJ laser pulse with a signal-to-noise ratio of 40:1 (32 dB) on a mild steel block with a surface temperature of 810°C (1490°F). Similar results were also obtained on a stainless steel sample.
3. No degradation of performance was observed after the probe had been repeatedly held in contact with hot steel for time intervals that ranged from 60 to 90 s for each contact even though no active water cooling was employed. It now appears relatively straightforward to develop EMAT's for semicontinuous use at temperatures up to 1300°C.

ADDENDUM

Since this AISI/NBS program was completed, Battelle Northwest Laboratories contracted Magnasonics to assemble an improved EMAT for measuring the transit time of ultrasonic waves through 9" thick sections of steel. Here, again, a pulsed laser was used as the ultrasonic transmitter but the improved EMAT receiver used a pulsed electromagnet instead of samarium-cobalt permanent magnets and was capable of continuous operation next to the hot steel because it was housed in a water cooled, ceramic housing. Preliminary results show that this EMAT put out broad bandwidth signals with 20 dB signal-to-noise ratios on 9" thick stainless steel samples with surface temperatures of 2000°F. Signals were still observable when the EMAT air gap was over 1/4".

ACKNOWLEDGEMENTS

The help and assistance of F. Mauer and J. Martinez (NBS) are gratefully acknowledged.

REFERENCES

1. H. N. G. Wadley, *J. of Metals*, Oct. 1986.
2. C. B. Scruby, R. J. Dewhurst, D. A. Hutchins, and S. B. Palmer, Research Techniques in Nondestructive Testing V, ed., R. S. Sharpe, p. 281, Academic Press, Oxford (1982).
3. H. N. G. Wadley, C. K. Stockton, J. A. Simmons, M. Rosen, S. D. Ridder, and R. Mehrabian, Review of Progress in Quantitative NDE 1, p. 421, Plenum Press, New York (1982).
4. H. N. G. Wadley, J. A. Simmons, and C. Turner, Review of Progress in Quantitative NDE 3B, p. 683, Plenum Press, New York (1984).
5. E. P. Papadakis, et al., J. Acoust. Soc. Am. 52, p. 855 (1972).
6. C. F. Vasile and R. B. Thompson, Ultrasonics Symposium Proceedings, IEEE Cat. No. 77CH1264-ISU, p. 84 (1977).

NONCONTACT LASER ULTRASONIC SYSTEM FOR INSPECTION OF HOT STEEL BODIES DURING PROCESSING

MOSHE ROSEN AND ROBERT E. GREEN, JR.

Center for Nondestructive Evaluation
and
Materials Science and Engineering Department
The Johns Hopkins University
Baltimore, MD 21218

ABSTRACT

The objective of this paper is to demonstrate the capability of a noncontact laser ultrasonic generation and detection system for detection of primary pipe and gross porosity in hot steel slabs, blooms, and billets and to map the location of the defects during processing. Ultrasonic pulses are to be generated on one surface of a hot steel slab by impingement of a single-pulse from a high energy laser. The ultrasonic pulses propagating in the slab can be detected on both the same side as the generator (pulse-echo) and on the opposite side (through-transmission) by means of a laser interferometer incorporating a helium-cadmium laser. Assembly of the generation and detection subsystems on a scanning device permits rapid monitoring of the desired volume of the hot slab. The approach also affords the possibility of acquiring information useful for material characterization and processing.

INTRODUCTION

Pipe, or shrinkage cavity is a result of the present practice of the steelmaking process (Ref. 1). As the molten steel solidifies within an ingot mold, evolution of gases and thermal contraction during solidification cause the formation of cavities primarily at the top of the ingot. As the internal surfaces of the cavity are exposed to the atmosphere, oxide layers are formed. Upon subsequent deformation of the ingot, e.g., rolling, the oxide coating of the cavity prevents its welding. These internal discontinuities, of a permanent nature, are highly detrimental to the quality of the rolled material, and must be cropped off. The cropping operation is presently a manually controlled process. The operator visually inspects the steel slab and determines the appropriate cropping location based on his acquired experience. Quite often, the cropping operator shears off several slices before he is satisfied that all pipe has been removed from the top of the ingot. Also, in some cases an overly conservative operator shears off excessive good material in order to assure removal of the internal discontinuities. Such a procedure has proven to be costly and time consuming. It is believed by technical executives of the steel industry in the U.S. and worldwide that the cropping operation would be optimized if the operator could receive

information from an automatic inspection system capable of detecting and locating pipe and gross porosity within the slab or bloom. This would render the cropping process more efficient, reliable and independent of human error (Ref. 2). An automatic detection and location system would enhance productivity by diminishing labor and energy intensive operations, and by improving the quality assurance of the final product.

A substantial investigative effort, worldwide, was devoted to solve this problem (Ref. 3-11). A wide variety of techniques was examined for feasibility, e.g., online x-ray radiography, gamma-ray tomography, eddy currents, electromagnetic ultrasound transduction (EMATS) and contact ultrasonic methods. In Europe, USSR, Japan and France, and to some degree in the USA, the main effort was addressed toward conventional ultrasonic techniques whereby an array of ultrasonic transducers is subjected to a momentary forced contact with the hot slab. Water spray precedes the contact, thus affording an acoustic coupling between the transducers and the steel slab and localized cooling of the slab in order to prevent overheating of the ultrasonic transducers. In spite of the substantial technological effort, the conventional bulk ultrasonics technique has met with limited success only on a laboratory scale. The pressure-coupled ultrasonic transducers have never been applied for full production. The major steel companies in the world are actively engaged in searching for a more efficient means to assess the internal soundness of the material (Ref. 2).

The purpose of this paper is to describe a sensing system for online monitoring and control of the internal soundness of steel slabs and blooms at elevated temperatures by means of noncontact ultrasonic techniques employing laser devices for both generation and detection of ultrasonic waves.

LASER GENERATION OF ULTRASOUND

Application of a transient load on the surface of a metal by means of rapid energy deposition from a single-pulse Q-switched high energy laser produces a thermoelastic compressive stress wave that propagates through the material. Rapid deposition of laser energy into absorbing material produces a state of unbalanced compressive thermal stress as the heated materials wants to expand but is restrained initially by its own inertia. The thermoelastic mechanism for generation of acoustic waves is based on the solution of the wave equation of forced oscillations of a material under the effect of a thermoelastic force. The amplitude of the acoustic oscillation is given by the generalized equation of thermoacoustics (Ref. 12) containing expressions in terms of the amplitude of surface displacement, sound wave velocities of compressional and transverse mode of propagation, temperature dependence of heat conductivity and thermal expansion coefficients, elastic moduli of the material, and the temperature field distribution.

The use of lasers to generate ultrasonic pulses at metal surfaces was first discussed by White (Ref. 13). His analysis considered the expected temperature rises and the temperature profiles generated in the metal as a result of laser beam irradiation. Later work (Ref. 14) predicted the form of the stress pulse likely to be generated once the temperature distribution was determined (Ref. 15). Two regimes were considered. The first is the generation of plane elastic waves by thermal expansion at the free and constrained surfaces due to thermoelastic compressive stresses. The second regime is the formation of plasma, at very high laser power densities, resulting in ablation which imparts a momentum impulse to the metal surface. In general, the heating times are considered to be very short; thus, thermal diffusion can be neglected. The displacement of the front surface depends on the velocity of material expansion that produces the sound wave and the penetration depth of the stress pulse (Ref. 16). For a laser power density of approximately 1 MW/cm^2 and pulse duration of 30 ns, the free surface displacement is of the order of 1 \AA . At higher power densities, of the order of 100 MW/cm^2 , some of the material will be removed by ablation when the surface temperature reaches the vaporization point. Since the time to raise the surface temperature to vaporization is relatively long, even for such high power densities (about 100 ns), the amount of material removed by ablation is negligible.

Ready (Ref. 17) has shown the temperature distribution obtained with laser generation of ultrasonic pulses. Solution of the one-dimensional heat diffusion equation shows that a short high-power density pulse leads to a higher peak surface temperature than a longer, low-power density pulse of identical total energy.

The amplitude of longitudinal, transverse and Rayleigh surface waves generated at free metal surfaces by a Q-switched Nd:YAG laser operating at 1.06 \mu m has been investigated by Aindow et al. (Ref. 18). The acoustic source formed by irradiation of a free metal surface may be approximated as a thin metal disc. For a source situated deeper in the materials, compressional waves in all directions would be generated. For constrained surfaces, the stresses normal to the surface become dominant resulting in an increase in the generation efficiency of longitudinal waves. When the laser intensity is sufficiently high to cause ablation, the impulse force given to the surface by the vaporization process enhances the amplitude of the longitudinal wave, similar to the situation occurring with a constrained surface in the thermoelastic regime. The Q-switched Nd:YAG laser produced single pulses with a duration of about 20 ns with energies up to 200 mJ. Aindow et al. (Ref. 18) found that a laser pulse energy of 5 mJ produced a 2 mV signal from a 33 MHz longitudinal piezoelectric transducer receiver located on the opposite side of a 1" thick sample of aluminum. For power densities in the thermoelastic regime, a linear relation was obtained between the laser energy

deposition and the receiver transducer output. Plasma was formed at the metal surface when the laser was focused, thereby achieving increased efficiencies in the longitudinal wave pulse generation. Such an enhancement is not expected for the generation of transverse waves since such momentum effects are not a shear generation mechanism. Hutchins et al. (Ref. 19) have observed an enhanced efficiency of longitudinal pulse generation, up to a factor of 40 dB, by application of a constraining overlay. Surface contamination, such as films and oxide layers, may also enhance the generation of acoustic pulses. The energy deposited by a Q-switched laser, on the surface of a metallic sample will be absorbed within the skin depth of the metal at the irradiating wavelength; however, some thermal diffusion may occur over the time duration of the laser pulse, thus giving rise to a temperature distribution in a localized small volume. It was shown, however, that significant temperature rises within the material would not exist at distances exceeding 10 μm from the surface, even after 100 ns from the nominal pulse irradiation (Ref. 12,15).

One of the earliest applications of laser-generated ultrasound for flaw detection was that of Bondarenko et al. (Ref. 20) who used a Q-spoiled ruby laser emitting single pulses with widths of 30-50 ns and power up to 50 MW. Calder and Wilcox (Ref. 21) used a single-pulsed, Q-switched ND:glass laser at energies up to 15J with typical pulse duration of about 30 ns. Very strong ultrasonic echoes were observed but the 15 J laser pulse caused significant surface damage on polished metallic samples. A focused beam from a ND:YAG laser with a 17 ns pulse duration and an intensity of 40 mJ was applied to perform nondestructive testing on microwelds (Ref. 22).

The risetime of a laser induced elastic wave is comparable with the risetime of the laser pulse. Availability of such a sharp leading edge suggests the possibility of high precision measurements of the velocity of propagation of acoustic waves. Generation of elastic waves, by means of a Q-switched Nd:YAG laser with a 2 mJ pulses, has been used to measure the velocity of extensional waves in metallic glass ribbons subjected to controlled heat treatments and thus determine the kinetics and mechanism of crystallization (Ref. 23). The elastic waves propagated along a 200 mm distance were detected by a 10 MHz quartz transducer.

LASER DETECTION OF ULTRASOUND

Propagation of ultrasonic waves in a medium causes surface displacements that can be measured optically by exploiting the phase shift of an optical beam reflected from the surface of the material. When the reflected beam is appropriately combined with a reference optical beam, from a helium-neon laser, phase changes are converted into amplitude changes that are detectable by a suitable photodiode. These amplitude changes are

proportional to the surface displacements on the test sample when an ultrasonic wave is propagating through it.

Interferometry has been used to measure very small surface displacements as early as 1900. However, with the advent of lasers, supplying stable and intense coherent light sources, laser interferometry became an important analytical tool. The mode of operation of an interferometer, e.g. the Michelson type, is as follows: Light from a coherent monochromatic source is divided by means of a beam splitter into two secondary beams. One of these secondary beams travels towards the test sample surface. The other beam is directed towards a reference mirror located at a fixed distance from the beam splitter. The two reflected beams are recombined at the beam splitter, as they return from the reference mirror and test sample, respectively. The recombined beam is detected by an appropriate detector, e.g., a photodiode. Because the secondary beams originate from the same source, the laser, sharp interference fringes are produced at the detector. The number of fringes is a measure of the optical path difference between the two secondary beams. For small changes, less than a wavelength, the variation in fringe intensity corresponds to the relative change in position of the surface of the test sample, since the fringe intensity varies sinusoidally as a function of the optical path difference. A high sensitivity photomultiplier translates the changes in intensity to changes in amplitude, or distance.

External noise introduced by mechanical or thermal vibrations may cause relative changes in the optical path length. However, these noise signals normally occur at very low frequencies relative to the ultrasonic frequencies under consideration (1-10 MHz). Apparent path differences may also arise from relative motion among the optical components of the interferometer, and even from pressure and temperature fluctuations of the ambient air. Any specimen motion also shifts the constant path difference and may displace the fringe pattern, or change the intensity of the detected recombined beam.

The Fizeau design of an interferometer alleviates part of the difficulties. To compensate for the random fringe motion so as to maintain maximum sensitivity the quadrature dual technique is used (Ref. 24,25). The input laser beam after expansion and collimation is plane polarized and then resolved into two components by means of a phase retardation plate, $\lambda/8$. The parallel component is delayed by 45° with respect to the perpendicular component. Upon transmission of the returning beams through the retardation plate for a second time, the phase difference becomes 90° , corresponding to circularly polarized light. Thus, a shifted interference pattern is obtained. In addition, the square root of the sum of the squares of the high frequency components (orthogonal to each other) yields the same signal (except for the phase) as would the ideal path difference $\lambda/4$. Thus, the low frequency random fringe

shift is automatically compensated for if both outputs are recorded. Maximum sensitivity is obtained for any value of the ideal path difference. Such an interferometer was constructed for determination of changes in elastic properties and ultrasonic attenuation in rapidly solidified microstructures (Ref. 26, 27). Figure 1 shows a schematic representation of this system.

Stabilization of the interferometer against low frequency mechanical vibrations can be achieved by an electromechanical feedback arrangement (Ref. 28, 29). The reference mirror is attached to a piezoelectric device. The signal from the detector is filtered into high and low frequency components. The low frequency component is the mechanical noise. The noise signal is applied to a feedback circuit that charges or discharges a capacitor that drives the piezoelectric mirror mount to eliminate the noise signal. For this type of apparatus, displacement sensitivities of about $0.5 \text{ }^\circ\text{A}$ are easily achieved (Ref. 28), which is adequate for most NDE applications involving displacements of the order of $0.5 - 20 \text{ }^\circ\text{A}$.

Compared with other sensors, interferometers offer several advantages. The sensitive area is definite, and can be made as small as a few microns in diameter for highly localized detection. The measured quantities are displacement and phase. Independent methods of calibration are applicable. The bandwidth that determines the fidelity of reproduction of signal waveshapes is limited not by the physical nature of the transduction process but by the associated electronic components. In this respect, performance can exceed that of conventional piezoelectric transducers. Small signal resolution and bandwidth being related, displacements of a few $^\circ\text{A}$ are detectable at 20 MHz bandwidth.

DETERMINATION OF DEFECTS IN HOT STEEL BODIES DURING PROCESSING

It is not clear as yet which type of these laser systems possesses the features necessary for optimization of a practical system. The desired intensity of the laser-generated ultrasonic pulse depends to a large extent on the absorption of the acoustic waves in the test sample. The required generation intensity will thus affect the basic parameters of the laser detection device. Among the features to be assessed should be the size and weight of the laser, ruggedness of construction, power requirements, pulse power and repetition rate, tube life at operating power level, and cost.

Several state-of-the-art laser beam interferometer detectors of acoustic waves propagating through metallic solids have been constructed and employed at Johns Hopkins, the Royal Military College (Canada), and at the National Research Council of Canada (Montreal). The most recent of these possesses a frequency bandwidth of 60 MHz and the capability of routinely detecting waves possessing amplitudes as small as $1 \text{ }^\circ\text{A}$. Because of this

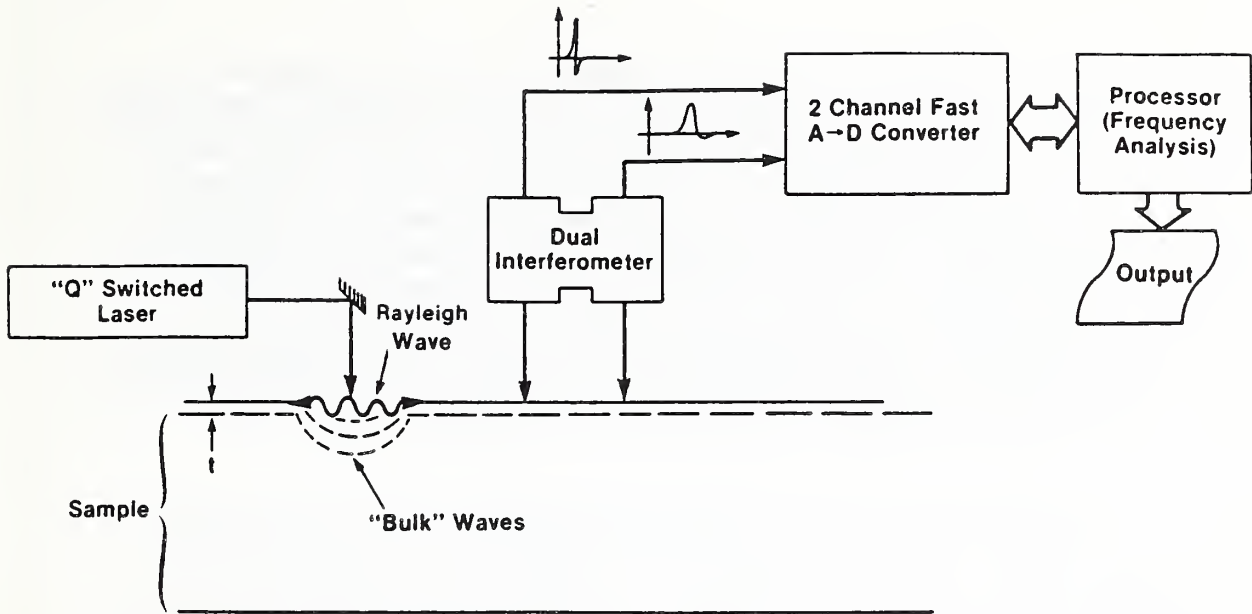


Fig. 1. Laser-beam generation and dual-laser interferometric detection of surface and sub-surface ultrasonic waves.

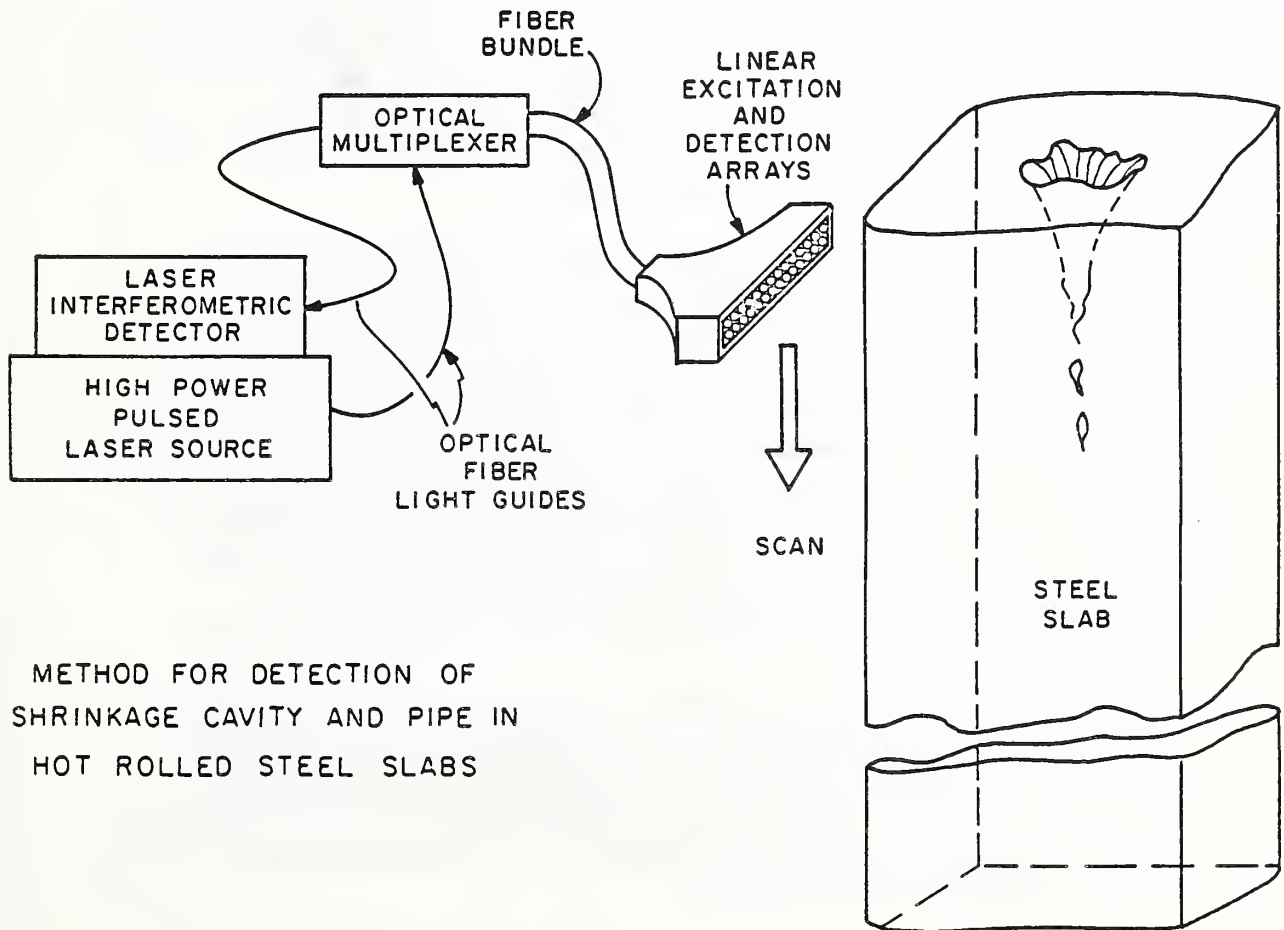


Fig. 2. Non-contact laser generation/detection ultrasonic system for inspection of hot steel bodies during processing.

experience, and because of preliminary measurements comparing the reflectivity of red laser light (helium-neon) with that of blue-green laser light (argon) from a red hot steel bar, it would be profitable to construct a laser beam interferometric ultrasonic wave detector incorporating a blue-green laser. A laser operating in this blue-green wavelength regime is required since measurements have shown that the signal-to-noise ratio of a red laser beam interferometers, as used in all prior interferometers, is severely degraded when used as a detector with a red hot steel body. The reason for this degradation is that some of the energy radiated by the hot steel matches the wavelength of the laser itself. The use of a blue-green laser greatly improves the signal-to-noise ratio under similar circumstances.

In the past, argon lasers have been used exclusively in the blue-green wavelength range, but recently developed helium-cadmium lasers offer many advantages. When an argon laser is operated at its maximum power, tube lifetime is only about 1,500 hours. A helium-cadmium laser operating at full power is expected to have a tube lifetime of 4,000 hours. The electrical efficiency of a helium-cadmium laser is five or six times that of an air-cooled argon laser. Not only do helium-cadmium lasers lower electricity bills, but more importantly, the cost of a replacement will be significantly greater. Because argon lasers require higher discharge current (and lower discharge voltage) than helium-cadmium lasers, they tend to exhibit greater line ripple, unless specially corrected for. Although argon lasers are usually shorter than similarly powered helium-cadmium, helium-cadmium lasers are significantly lighter. These many advantages make helium-cadmium the laser of practical choice for the proposed research.

For the purpose of identification of the specific laser systems for generation and detection of ultrasonic waves in hot steel slabs, the effect of nonadherent oxide layers on the steel slabs should be evaluated. It is not at all obvious that an oxide layer (scale) on the surface of the steel slab will interfere with the ultrasonic measurement. The mechanical and physical properties of the oxide layer, e.g. temperature, ductility, thickness, adherence to the surface, etc., determine whether the presence of an oxide layer is beneficial or not. In certain cases, where a compatible laser irradiation is generated, such a layer may act as an artificial overlay on the irradiated surface to produce a shock wave in the test sample. Under these circumstances, the generated ultrasonic pulse will be highly enhanced.

A series of experiments, properly designed and executed, should provide the necessary information for the evaluation of the noncontact methodology. This methodology has a great potential that should be exploited, particularly for solving the important problem that has eluded any realistic solution so far, namely, the inspection and characterization of hot steel bodies during actual processing.

Noncontact ultrasonics, employing laser generation and laser interferometric detection of sound waves can be remotely operated by means of optical fibers. Thus, the delicate instrumentation (lasers, etc.) can be located several hundred yards away from the steel processing halls. Furthermore, ultrasonic signals can easily be digitized and fed back into monitoring and control units of the metal processing systems. Therefore, a high degree of automation can be achieved while improving the reliability, quality assurance and profitability of the hot processing of steel. Figure 2 shows a schematic presentation of such a noncontact laser generation/detection ultrasonic system for inspection of hot steel bodies during processing.

REFERENCES

1. H. E. McGannon, "The Making, Shaping, and Treating of Steel", U.S. Steel Corporation, Ninth Edition, Herbiem and Held, Pittsburgh, PA. (1971).
2. "Research Needs for Process-Control Sensors", American Iron and Steel Institute General Research Committee--Task Group on Steel-Industry Research Priorities for Process Control and Sensor Development (January 1981).
3. B.E. Droney and T. J. Pfeiffer, Materials Evaluation, **38**, 1130 (1981).
4. R. C. Booth and R. N. Cressman, Materials Evaluation, **39**, 1130 (1981).
5. E. P. Papadakis, L. C. Lynnworth, K. A. Fowler and E. H. Carnevale, J. Acoust. Soc. Am. **52**, 850 (1972).
6. K. R. Whittington, British J. NDT, **242** (1978).
7. K. Miyagawa et al., "Nondestructive Testing Systems for Pipe and Tube Mills at Nippon Corp.", Nippon Steel Techn. Report No. 14 (1979).
8. J. M. Mandula, Materials Evaluation, **30**, 49 (1972).
9. K. G. Bergstrand and P. Nilsson, Iron and Steel Engineer, **57**, 1 (1980).
10. J. Pachtem and J. Cornet, "Resultats Pratiques d'une Gammagraphie en Exploitation Industrielle", Commission des Ingenieurs de Laminoirs, (Feb. 1968).
11. J. C. Albert, J. Dumont-Fillon and J. Pinaud, Proc. 8th World Conf. on NDT, Cannes, France, (Sept. 1976).
12. J. F. Ready, J. Appl. Phys. **36**, 462 (1965).
13. R. M. White, J. Appl. Phys. **34**, 3559 (1963).
14. L. S. Gournay, J. Acoust. Soc. Am. **40**, 1322 (1966).
15. A. M. Aindow, R. J. Dewhurst, D. A. Hutchins, and S. B. Palmer, in 1980 European Conf. on Optical Systems and Applications, Utrecht, Holland 1980, European Conf. Abst. Vol. 41, Paper N6.
16. J. C. Bushnell and D. J. McCloskey, J. Appl. Phys. **39**, 5541 (1968).

17. J. F. Ready, "Effects of High Power Laser Radiation", Academic Press, New York (1971).
18. A. M. Aindow, R. J. Dewhurst, D. A. Hutchins and S. B. Palmer, J. Acoust. Soc. Am. **69**, 449 (1981).
19. D. A. Hutchins, R. J. Dewhurst, S. B. Palmer, Ultrasonics, **19**, 655 (1976).
20. A. N. Bondarenko, Y. B. Drobot and S. V. Kruglov, J. NDT, **12**, 655 (1976).
21. C. A. Calder and W. W. Wilcox, Mater. Evaluation, **38**, 86 (1980).
22. Y. Bar-Cohen, J. NDT, **21**, 76 (1979).
23. M. Rosen, H. N. G. Wadley and R. Mehrabian, Scripta Met. **15**, 1231 (1981).
24. E. R. Peck and S. W. Obetz, J. Opt. Soc. Am. **43**, 505 (1953).
25. D. Vilkomerson, Appl. Phys. Lett. **29**, 183 (1976).
26. M. Rosen, C. H. Palmer and S. Fick (private communication).
27. M. Rosen and E. Horowitz, The Johns Hopkins University, Center for Materials Research Report CMR-NDE 7 (Sept. 1982).
28. C. H. Palmer and R. E. Green, Jr., Appl. Opt. **16**, 2333 (1977).
29. C. H. Palmer and R. E. Green, Jr., in "Nondestructive Evaluation of Materials", J. J. Burke and V. Weiss, editors, pp. 347-378, Plenum Press, NY (1979).

Impedance of a Coil in the Vicinity of a Crack

Arnold H. Kahn

National Bureau of Standards, Washington, DC 20234

Calculations are presented for the impedance of a coil as it is moved in the vicinity of a v-groove crack in the surface of a metallic slab. The coil is modeled as a pair of parallel wires, oriented parallel to the crack, carrying equal and opposite currents. The inhomogeneous electromagnetic fields in the air above the slab and in the metal are determined by the boundary integral equation (BIE) method. This approach leads to a pair of coupled integral equations for the tangential components of the electric and magnetic field vectors on the surface of the slab containing the crack. The solutions, which are obtained by standard method of discretization, are valid for arbitrary ratio of crack or coil dimensions to skin depth. Illustrations are presented of the Poynting vector distribution over the surface of the metal, including the crack faces. A plot of the complex impedance is given in the form of a coil scan across the crack.

1. Introduction

In the design of electromagnetic NDE systems for the detection and examination of cracks or other defects in conducting materials, it is necessary to have a quantitative description of the electric and magnetic fields in the vicinity of the defect. In practice, the fields are produced by an exciting coil, the impedance of which is used to provide the detection signal. (The voltage induced in a secondary pickup coil may also be used.) In previous work by the author [1,2], the fields in the vicinity of a crack were calculated for models based on excitation by a spatially uniform applied magnetic field such as would be found in the interior of a solenoid. The present work offers an improved description of the fields through the introduction of nonuniformity of the applied field due to finite coil size and the inclusion of coil position relative to the crack.

Recently there has been significant activity in the development of theoretical modeling in electromagnetic NDE. The finite element method has been applied by Ida and Lord [3] to the cylindrical

geometry of reactor tubing. Studies have been presented by Auld *et al.*, Kincaid *et al.*, Bahr, and other [4] on experimental and theoretical considerations of crack detection and coil design. A principal difficulty is the calculation of signals when the electromagnetic skin depth and crack size are of comparable magnitude, which is the domain of greatest sensitivity. The two-dimensional model of this paper represents a contribution toward the solution of this problem. A full three-dimensional treatment may be possible as new computing capabilities are developed [3].

2. Description of the Model and Theoretical Formulation

The calculations described in this paper are based on the following model: We consider a flat surface with an infinitely long, symmetrical v-groove representing a surface crack, the material is homogeneous and uniform in conductivity. A pair of wires carrying equal and opposite currents is located above the slab and is oriented parallel to the crack. The wires are infinitesimal in thickness and infinite in extent. This

simplified model of an eddy-current testing configuration allows a two-dimensional calculation of the impedance signals due to the crack. The calculation will allow for the effect of crack dimensions; coil dimensions, elevation, and displacement; and the material parameters of the metal. This is an improvement over calculations in which the exciting field is spatially uniform.

By solving for the electromagnetic fields first on the surface of the metal and then at the exciting wires, we obtain the impedance due to the presence of the metallic region. If the problem is solved for a plane surface without the crack, then the additional impedance due to the crack may be obtained by subtraction. Also, by solving for different positions of the wires representing the detection coils, we may obtain the impedance signal on traversing the crack and also the signal due to liftoff effects.

The model is illustrated in figure 1. The circles above the surface represent the wires, with + and - indicating the direction of the impressed current $I_0 e^{-i\omega t}$, where ω is the angular frequency and t the time. The current is held at fixed amplitude I_0 , according to the usual procedure for eddy-current NDE. In the figure additional parameters are shown: A is the separation between the wires, H is the height of the coil above the plane, P is the center position of the coil relative to the crack, D is the depth of the crack, and F is the half-width of the crack opening.

Because of the symmetry of this two-dimensional model, the electric and magnetic fields may be derived from a vector potential, A , which has only one component, A_z [5], where the z -direction is parallel to the wires and the crack. If the wires were not parallel to the crack, a full three-dimensional analysis would be

necessary. The vector potential is thus of the form $A(x,y)e^{-i\omega t}$, where A is complex to represent phase relations with respect to the exciting current.

In the region above the conductor the vector potential satisfies a Helmholtz equation. However, at the frequencies of eddy current testing the transit time for wave propagation across the region of the crack is negligibly small and a quasi-static approximation is satisfactory. Thus, in the region above the metal slab the vector potential satisfies the Laplace equation,

$$\nabla^2 A = 0, \quad (1)$$

except for the singularities at the wires. Below the surface, in the metallic region, the Helmholtz equation is obeyed,

$$(\nabla^2 + k^2)A = 0, \quad (2)$$

where

$$k^2 = i\sigma\omega\mu \quad (3)$$

is the square of the propagation constant, σ is the electrical conductivity, and μ is the magnetic permeability. Here too, displacement currents are neglected, in this case because the ohmic currents represented by the k^2 term are so much larger. At the boundary surface, including the faces of the crack, the

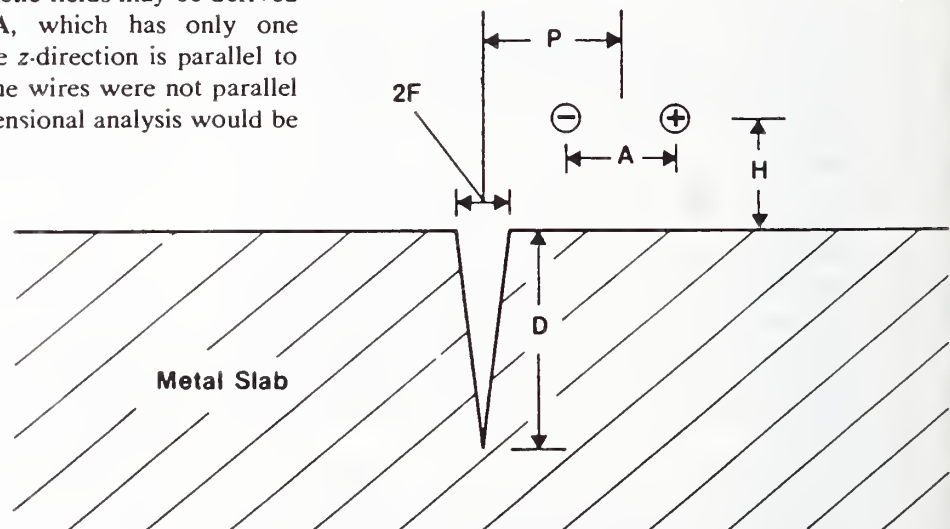


Figure 1-Configuration of model and parameters for the calculation of the impedance signal due to a crack.

- | | | | |
|-----------|----------------------|----------|--|
| D | Crack Depth | A | Wire Separation |
| 2F | Crack Opening | H | Wire Elevation |
| | | P | Wire Position Relative to Crack |

usual conditions of continuity of tangential E and H , and normal B and D must hold. In terms of the vector potential, these conditions are equivalent to the continuity of A and $1/\mu \partial A/\partial n$, where $\partial A/\partial n$ is the normal derivative of A at the interface. To summarize, the vector potential must satisfy the Laplace equation in the upper region, the Helmholtz in the lower region, and conditions of continuity at the interface, and it must approach the known form of the impressed field in the vicinity of the source wires.

The method of solution selected in this paper is an extension of the boundary integral equation (BIE) approach [6,7]. This method, usually applied to a single region, has been used by the author [2] in eddy-current problems involving excitation by a uniform ac field. In the present application the method leads to a pair of coupled Fredholm integral equations of the first kind, as follows:

By application of Green's theorem we express the vector potential in the upper region in terms of the source fields and the values of A and its normal derivative $\partial A/\partial n$ on the bounding curve:

$$A(r) = \mathcal{S}(r) + \int \frac{\partial G(r, S')}{\partial n'} A(S') dS' - \int G(r, S') \frac{\partial A(S')}{\partial n'} dS'. \quad (4)$$

in which dS' is an element of arc in a planar cross-section normal to the surface of the metal. In the above, \mathcal{S} is the vector potential due to the source wires as if the metallic region were absent. The two integrals give the change due to the induced currents below the boundary. They are taken over the boundary \hat{n} is the unit normal vector pointing out of the upper region. The remaining boundary closure at infinity makes no contribution since the fields decay with sufficient rapidity. Green's function for the Laplace operator is given by

$$G(r, r') = -1/2\pi \log|r-r'|; \quad (5)$$

it satisfies

$$\nabla^2 G(r, r') = -\delta(r-r'), \quad (6)$$

where δ is the two-dimensional Dirac delta function. For the two-wire case treated in this paper, the source field S has the form

$$S(r) = I_0[G(r, r_+) - G(r, r_-)],$$

where r_+ and r_- are the positions of the wires which

carry the exciting current, I_0 , parallel and anti-parallel to the z -direction, respectively. In the metallic region

$$A(r) = - \int \frac{\partial \mathcal{G}(r, S')}{\partial n'} A(S') dS' + \int \mathcal{G}(r, S') \frac{\partial A(S')}{\partial n'} dS', \quad (7)$$

where \mathcal{G} is now the two-dimensional Helmholtz Green's function,

$$\mathcal{G}(r, r') = (i/4)H_0^{(1)}(k|r-r'|), \quad (8)$$

where $H_0^{(1)}$ is the Hankel function of the first kind, order zero. It, too, has a logarithmic singularity and satisfies the Helmholtz equation with a source,

$$(\nabla^2 + k^2) \mathcal{G}(r, r') = -\delta(r-r'). \quad (9)$$

This latter Green's function contains the complex k and represents a damped outgoing cylindrical wave at large values of $r-r'$. In eq (7) we have retained the same direction of the normal vector \hat{n} ; hence the unusual sign convention on the right hand side.

The BIE method prescribes letting r approach the surface to obtain the fields on the bounding surface. When we let $r=S$, a well-defined expression is obtained if we use the Cauchy principal values for the singular integrals and replace A on the boundary by $A/2$. For nonmagnetic materials A and $\partial A/\partial n$ are both continuous across the boundary, and we shall so restrict the present calculations. The resulting BIE's are

$$\frac{1}{2}A(S) - \int \frac{\partial G(S, S')}{\partial n'} A(S') dS' + \int G(S, S') \frac{\partial A(S')}{\partial n'} dS' = \mathcal{S}(S) \quad (10)$$

$$\frac{1}{2}A(S) + \int \frac{\partial \mathcal{G}(S, S')}{\partial n'} A(S') dS' - \int \mathcal{G}(S, S') \frac{\partial A(S')}{\partial n'} dS' = 0 \quad (11)$$

This is a coupled pair of equations for unknowns $A(S)$ and $\partial A(S)/\partial n$ on the interface. We may look on the

inhomogeneous term $\mathcal{S}(S)$ as the driving force for the system. When A and $\partial A/\partial n$ are found on the boundary, then the field A may be constructed at any point above the interface by application of eq (4), or below the interface by application of eq (7).

The ultimate objective is the determination of the impedance per unit length induced in the wires by the presence of the metallic region. The time-average of the power per unit length delivered by the exciting wires is given by the complex expression

$$P = \frac{1}{2} \int E' \cdot J^* da,$$

where J is the (constant) current density in the wires, E' is the electric field at the wires produced by the induced currents, and da is an element of cross-sectional area normal to the wires. E' is derived from the vector potential A' of the induced currents,

$$A' = A - \mathcal{S},$$

by the usual relation

$$E' = i\omega A'.$$

Hence, for a set of idealized line-wires, denumerated by the index i , we have

$$P = \frac{1}{2} \sum I_i^* i\omega A'_i,$$

Connection with conventional circuit parameters can be made by expressing P in terms of the currents, voltages per unit length, and impedance per unit length of the wires. Under the constant current assumption of eddy current testing, we have

$$P = \frac{1}{2} \sum V_i I_i^* = \frac{1}{2} \sum I_i I_i^* Z_i,$$

where V_i is the voltage per unit length induced in the i th wire and Z_i is the extra impedance in the i th wire due to induced currents in the metallic region. Finally we obtain

$$Z_i = i\omega A'_i / I_i$$

for the impedance per unit length in the i th wire, caused by the induction. Now A'_i is evaluated at the i th wire and can be computed by use of Green's theorem after A and $\partial A/\partial n$ have been found on the interface. Thus we have a method of computing the extra impedance seen by each wire due to the presence of the metal below. These impedances may now be calculated with and without a crack being present.

3. Numerical Treatment

The coupled integral equations are solved by an application of the method of moments [8]. The solution is expressed as a linear combination of a finite set of basis functions with unknown coefficients. The coefficients are determined by requiring that the integral equations be satisfied at a number of points equal to the number of unknown coefficients; i.e., point-matching is used.

For the basis functions, the elements F shown in figure 2 were used, after the method of Harrington [8].

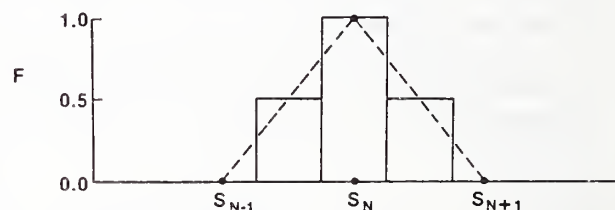


Figure 2—Triple-pulse hat function F used in the numerical calculations. The illustration shows the function $F(S-S_n)$. The dashed line is the common triangular hat-function.

We approximate the solution for the vector potential and its normal derivative on the interface by the finite sums:

$$A(S) = \sum A_i F(S-S_i) \quad (12)$$

and

$$\frac{\partial A(S)}{\partial n} = \sum N_i F(S-S_i) \quad (13)$$

These expansions are introduced into the integral equations, eqs (10) and (11). The integration over each element is carried out by use of the midpoint rule for the entire integrand of each flat section of the fundamental element, except when the Green's function is singular, i.e., when $S_i = S_j$.

When a singular integrand occurs in the evaluation of eq (10), the integration of the logarithmic Green's function is performed exactly. When a singular integrand occurs in eq (11), the dominant logarithmic part of the Hankel function is used for the evaluation.

The width of the elements is not restricted. It was found practical to use a fine grid where the solution

was large or varying rapidly, and a coarse grid elsewhere. With these approximations and the point-matching, the coupled integral equations are reduced to a linear algebraic system of the form:

$$\sum \left[\frac{1}{2} \delta_{ij} - \left(\frac{\partial G}{\partial n} \right)_{ij} \right] A_j + \sum G_{ij} \left(\frac{\partial A}{\partial n} \right)_j = \mathcal{S}_i \quad (14)$$

$$\sum \left[\frac{1}{2} \delta_{ij} + \left(\frac{\partial G}{\partial n} \right)_{ij} \right] A_j - \sum \mathcal{G}_{ij} \left(\frac{\partial A}{\partial n} \right)_j = 0 \quad (15)$$

In these equations, each doubly-subscripted term corresponds to that part of the integrations of eqs (10) and (11) connecting element j and matching-point i .

The calculations were first attempted with square pulse functions as the basis set. It was found that the solutions were unstable in the vicinity of the crack corners and near the location of a grid-size change. The use of the triple pulse element is equivalent to doubling the number of points in a pulse function calculation, but applying the constraint that the solution at each point be averaged with its two nearest neighbors. In addition to reducing the dimensions of the needed matrices, this has a smoothing effect and leads to solutions which are stable as the grid size is decreased. The triple pulse basis function may be looked upon as an approximation to the common triangular hat-function, shown in figure 2 by the dashed line. The hat-function yields a piecewise trapezoidal approximation to the solution which would be superior to the present form, but its application is precluded because of nonintegrability

when multiplied by the Hankel functions of the integrand. The solution of the linear equations was obtained by Gaussian elimination without pivoting. The logarithmic singularities of the Green's functions associated with the diagonal elements of the matrices allow this economical simplification. The solutions were considered to have converged when further refinement produced an insignificant change in the physical results, usually about 1 percent. Typically the dimension of the square matrices ranged from 200 to 300.

4. Coil Impedance in the Absence of a Crack

The radiation field of an oscillating dipole above a conducting earth was a problem first attacked successfully by Sommerfeld [9]. Analytical solutions have been given for finite coils by Dodd *et al.* [10,11]. These solutions are in the form of integrals over various Bessel function arguments. Numerical evaluation is possible; analytic evaluation is in terms of asymptotic series. The same methods can be applied to this problem of a pair of parallel wires over a plane. However, the approach of this publication is readily applicable in the absence of a crack. Solving an integral equation requires a greater computing effort than evaluating an integral solution for the lesser problem. However, it is quite useful to have the programs available as a byproduct of the crack case. In this section we examine the results of calculations for the parallel wire coil above a flat conducting half-space, calculated by the boundary integral equation method.

In figure 3 we show the results of a typical calculation. For this case, and all others reported here,

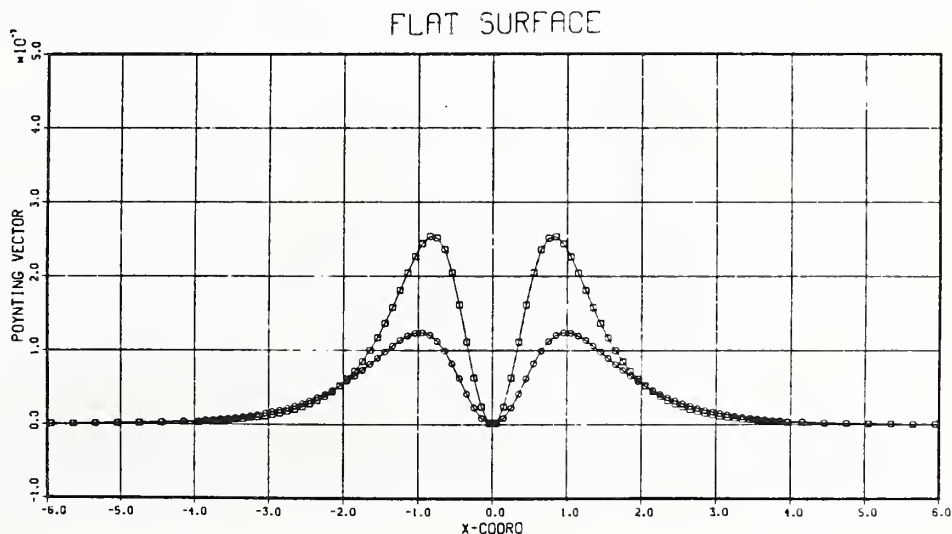


Figure 3—Poynting vector on the surface of a metallic slab in the absence of a crack. The coordinate x is along the flat surface of the metal. Distances are in units of the skin-depth and the Poynting vector is in units of $\mu_0 \omega 10^{-3}$. The exciting wires are located at $\pm 0.5 \delta$ and are at an elevation of 0.5δ .

lengths are in units of the skin depth δ , where

$$\delta = \sqrt{2/\sigma\omega\mu_0}, \quad (16)$$

and the symbols under the radical are the same as before. The complex Poynting vector \vec{S} , represents the time average of the complex energy flux, in our application, across the surface of the conductor. In the units we are using, we have

$$\begin{aligned} \vec{S} &= \frac{1}{2} \mathbf{E} \times \mathbf{H}^* \\ &= -\frac{i}{2} \frac{\mu_0 \omega}{\delta} \left| I_0 \right|^2 A \frac{\partial A^*}{\partial n'}, \end{aligned} \quad (17)$$

where A and $\partial A/\partial n'$ are calculated by solving the coupled boundary integral equations. While our principal interest is in the impedance change of the exciting wires, the Poynting vector plots show a detailed picture of the radiation field. The plots are useful for assessing the convergence of the calculations as well as for showing the regions of the test material where the significant absorption and field penetration take place.

5. Coil Impedance With a Crack

The presence of the crack adds two more parameters to the required inputs to the calculation. We treat only a symmetric v-groove crack which we specify by its depth and the half-width at its mouth. The calculations are performed in the same way as without the crack, with the only difference being that

the needed matrices are larger in dimension and somewhat more complex in preparation. The algorithms for the solution are identical to those of the previous case. The output of the program is the impedance per unit length of the wires, with the crack present. In addition we may inspect the complex Poynting vector on the surface of the crack as well as on the flat surface of the test material.

For the initial investigations we selected a crack depth of 2.0δ and an opening of half-width 0.25δ . The coil wires were taken as having a separation of 1.0δ and at an elevation of 1.0δ above the plane. These dimensions correspond to the physical situation of a No. 30 AWG wire insulated pair in close contact, elevated one radius above the contact with the plane, and driven at a frequency of 110 kHz. The relevant parameters for this model applied to aluminum are given in table 1.

Table 1. Parameters for model calculation based on aluminum at 110 kHz.

Resistivity	ρ	$2.82 \times 10^{-8} \Omega \cdot \text{m} (20^\circ \text{C})$
Conductivity	$\sigma (= 1/\rho)$	$3.54 \times 10^7 \Omega^{-1} \cdot \text{m}^{-1}$
Skin depth	δ	0.255 mm
Crack depth ($= 2\delta$)		0.51 mm
Crack half-opening ($\delta/4$)		0.064 mm
Wire radius ($\delta/2$)		0.13 mm

The calculations were performed for a range of values of the parameter P , the location of the coil center relative to the crack. Figures 4, 5, and 6 show the Poynting vector for the values $P=2.5 \delta$, 0.5δ , and 0.0

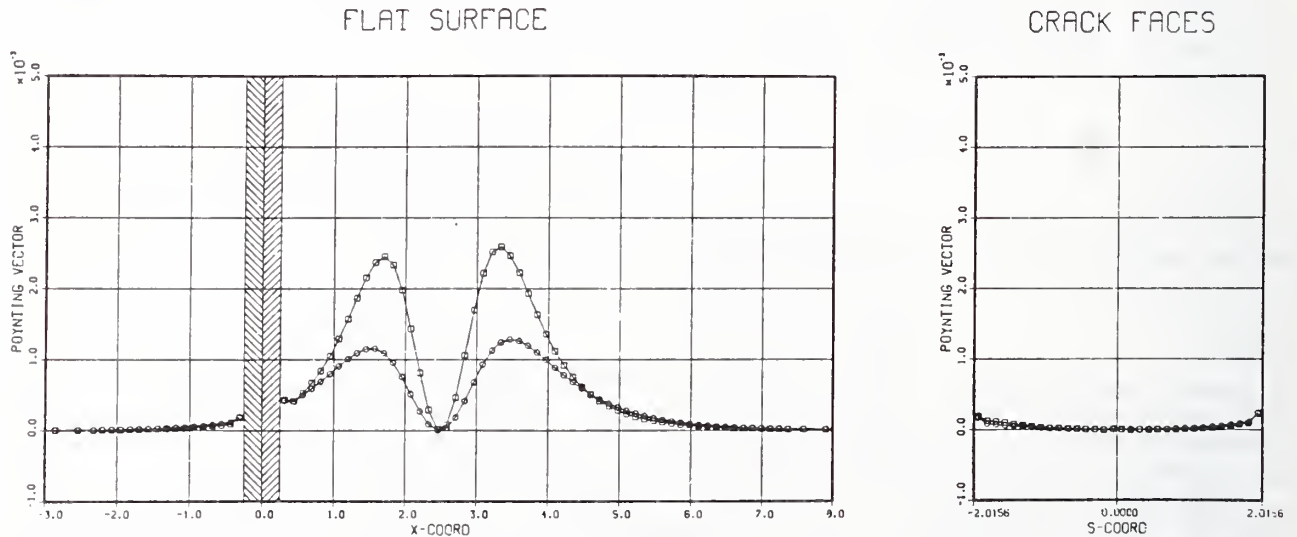


Figure 4—Poynting vector on the surface of a metallic slab with a crack. The coordinate S is along the faces of the crack, which is shown as folded open in the right-hand figure. The shaded band indicates the location of the v-groove crack. The lateral distance between the coil and the crack, P , is 2.0δ and the half-opening, F , is 0.25δ . All other parameters are as in figure 3.

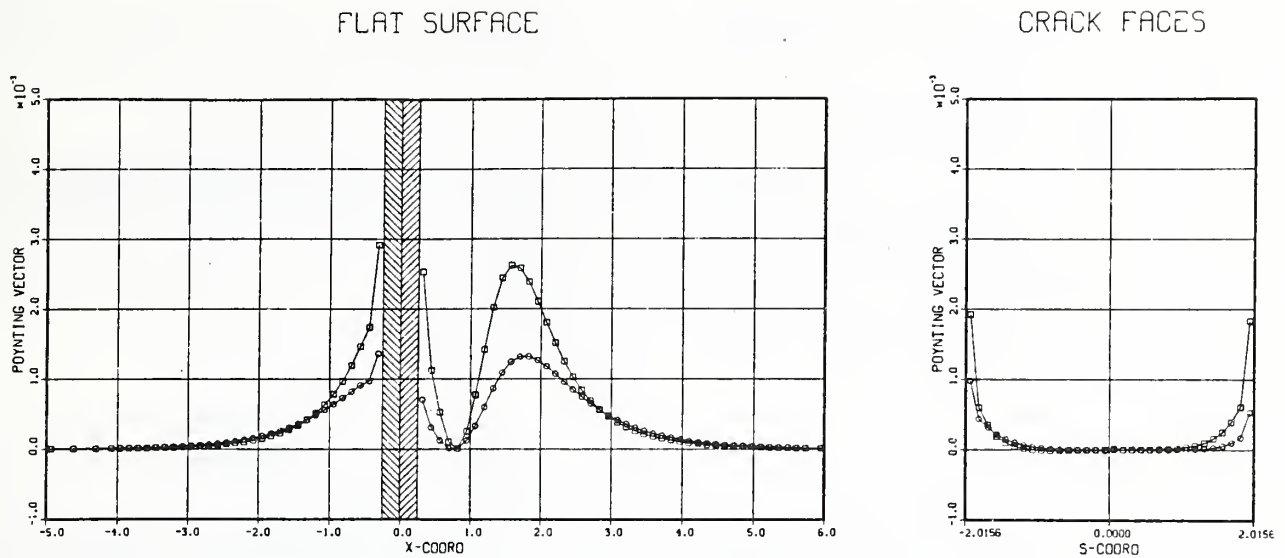


Figure 5—Poynting vector on the surface of a metallic slab with a crack. The lateral distance between the coil and the crack, P , has the value of 0.80δ ; all other parameters are as in figure 4.

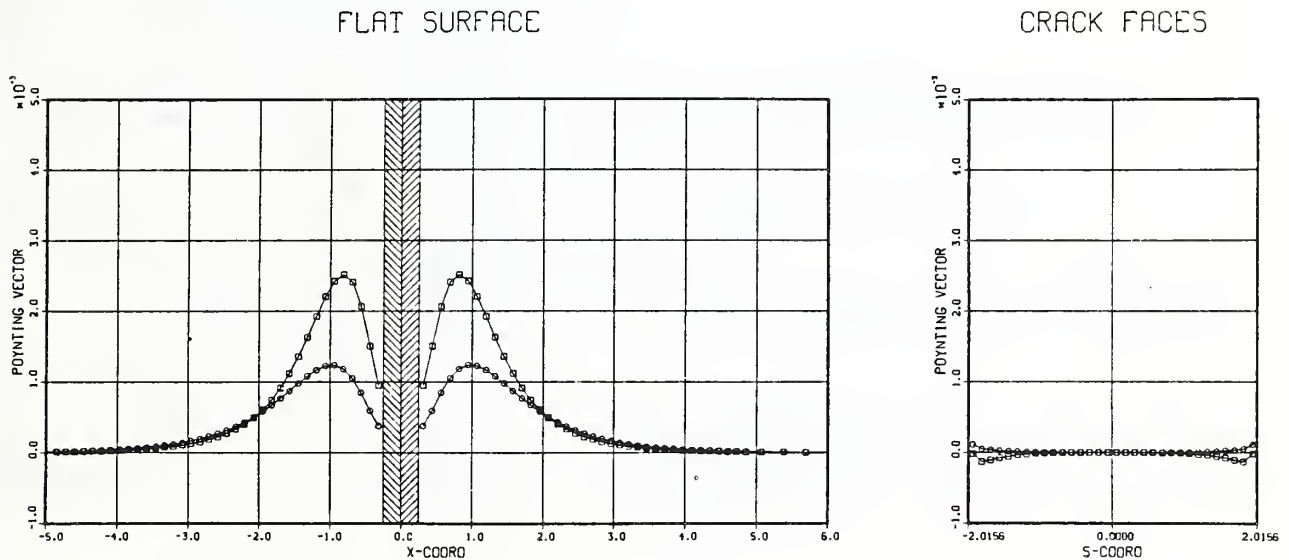


Figure 6—Poynting vector on the surface of a metallic slab with a crack. The lateral distance between the coil and the crack, P , has the value 0.0δ ; all other parameters are as in figure 4.

δ respectively, illustrating the deformation of the fields as the coil is brought up to the crack. These figures correspond to the same wire separation and elevation as in figure 3, the case with no crack.

Qualitative examination of the figures shows that in the presence of a crack, a portion of the integrated Poynting flux is "stolen" from the nearer of the peaks in the field distribution. The Poynting flux at the corners is somewhat increased over the value that would occur at that position if no crack were present.

Inside the crack, the Poynting flux decays to zero in approximately one skin-depth. This is quite the opposite behavior to that which occurs in the case of a uniform H -field parallel to the crack [2]. In that case, the Poynting vector is greatest at the tip and vanishes at the corners.

From a series of calculations like these, the coil impedance per unit length was obtained for numerous positions of the coil. The phase and magnitude of the impedance are shown in the plots of figure 7, in the

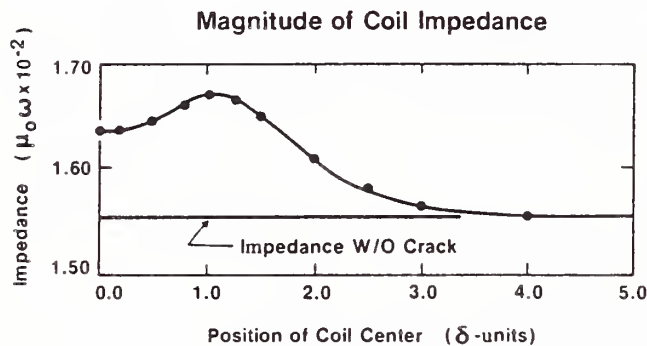
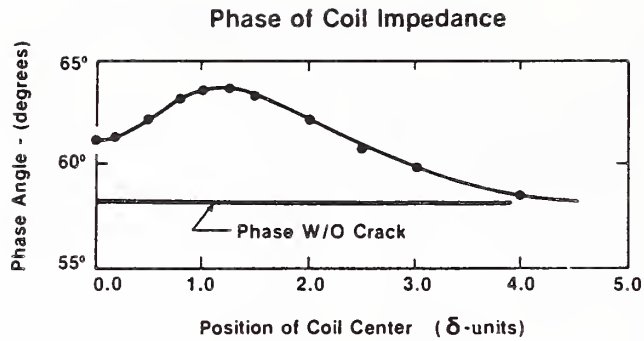


Figure 7—Plots of the phase and magnitude of the crack impedance signal as a function of the lateral displacement of the coil center relative to the crack. Parameters are as in figure 4.

form of a scan across the surface of the slab. These curves would be extended symmetrically for negative values of the coil displacement. The asymmetric signal obtained from an opposed pair of coils [12] can be

obtained from these curves by computing a differential scan corresponding to the coil pair separation.

The author wishes to express his thanks to Dr. B. Auld and Dr. C. Fortunko for most valuable discussions concerning crack detection. He is also grateful to Dr. S. Gershovits for interesting suggestions.

References

- [1] Kahn, A. H.; Spal, R.; Feldman, A. J. Appl. Phys. 48, 4454 (1977).
- [2] Kahn, A. H. in *Review of Progress in Quantitative Nondestructive Evaluation 1*, D. O. Thompson and D. E. Chimenti, eds., Plenum Press, New York, NY, p. 369.
- [3] Ida, N.; Lord, W. IEEE Computer Graphics and Appl. 3, 21 (1983).
- [4] *Review of Progress in Quantitative Nondestructive Evaluation 2*, D. O. Thompson and D. E. Chimenti, eds., (1983).
- [5] Landau, L. D.; Lifshitz, E. M. *Electrodynamics of Continuous Media*, Pergamon Press, New York, NY (1960), p. 121.
- [6] Rizzo, F. J. in *The Boundary-Integral Equation Method: Computational Applications in Applied Mechanics*, T. A. Cruse and F. J. Rizzo, eds., American Society of Mechanical Engineers, 1975, p. 1.
- [7] Jaswon, M. A.; Symm, G. T. *Integral Equation Methods in Potential Theory and Electrostatics*, Academic Press, London (1977).
- [8] Harrington, R. F. *Field Computation by Moment Methods*, Macmillan, New York, NY (1968).
- [9] Sommerfeld, A. *Partial Differential Equations in Physics*, Academic Press, New York, NY (1949), p. 236 et seq.
- [10] Dodd, C. V.; Deeds, W. E. J. Appl. Phys. 39, 2829 (1968).
- [11] Dodd, C. V.; Deeds, W. E.; Luquire, J. W. Int. J. Nondestructive Testing 1, 29 (1969).
- [12] Fortunko, C. M.; Padgett, S. A. Technical Activities 1982, Office of Nondestructive Evaluation, NBSIR 82-2617, p. 57 et seq.

3. WORKSHOP SUMMARIES

Three concurrent discussion groups (A, B, and C) were formed for consideration of the internal discontinuity problems that were most frequently encountered in the following hot areas:

Group A: Solidification

Group B: Intermediate Forming

Group C: Finishing

Discussion questions were provided for each group session. Each were discussed and conclusions were drawn concerning the priority of detection and the best sensor technology to explore.

3.1 **Solidification** - Chairman, J.R. Cook, ARMCO Inc.,
Recorder, H.N.G. Wadley, NBS

Question 1. What are the internal discontinuities of importance during continuous casting? Can they be prioritized on the basis of yield, controllability, feed forward/feedback control, quality?

- The general categories of internal discontinuities in prioritized order of importance during continuous casting are:

1. Inclusions
2. Cracks
3. Porosity (center looseness)
4. Center line segregation

- Calcium aluminum silicate inclusions in the 10 μm - 2 mm size range are the highest detection priority. Their occurrence is indicative of a breakdown in shroud gases just prior to casting. Smaller (<10 μm) aluminum oxide inclusions from aluminum killing are a less important detection priority. In either case, the appearance of significant inclusion concentrations flags a need for corrective action further back in the process and a region of unsound steel for future cropping. Corrective actions include adjusting shroud gas composition, ensuring correct degree of electromagnetic stirring, control of vortexing and avoidance of nozzle wear.

- Due to their difficulty of hot detection with today's technology, surface and subsurface cracks are, a major source of customer claims. They are responsible for extensive rework and downgrading of substandard product during downstream processing. Principal types of cracks encountered are:
 1. Starcracks: caused by a local excess of copper (pickup from mold). The cracks are starshaped, emanating along grain boundaries outward from the region of enhanced copper concentration.
 2. Oscillator cracks: surface cracks nucleated at the base of mold oscillator marks due to a local stress concentration. They are usually a manifestation of improper casting speed/cooling practice. They can also be caused by misalignment and bending.
 3. Surface Rip/Tears: infrequently encountered, usually due to poor lubricity in the mold.
 4. Longitudinal cracks: usually caused by poor heat transfer due to localized overcooling and sometimes misalignment.
 5. Subsurface cracks: longitudinal cracks, radial cracks and core cracks that may refill with steel forming potential internal discontinuities.
- Center looseness and shrinkage porosity may arise from an improper ratio of steel quantity to casting speed combined with the wrong cooling practice. Depending upon the severity, the condition sometimes can be corrected by subsequent reduction of cross sectional area.
- Center line segregation of nonmetallics may occur because of vortexing in conjunction with cooling of the liquid center. Usually electromagnetic stirring avoids the problem. If it is detected, it is a manifestation of an equipment malfunction, improper control of withdrawal speed and/or incorrect metallurgical length.

Question 2. Where do internal discontinuities occur during continuous casting? Can optimum sensor locations be identified for each type of discontinuity?

- The most deleterious inclusions form in liquid steel prior to its solidification. Teeming and other operations are used to reduce their concentrations to acceptable levels prior to entering into the mold. Mold fluxes then take over the role of entrapping and removing inclusions prior to solidification. Sensors located both to

monitor the efficiency of teeming and mold fluxing are required. The former would be located in the tundish, the latter near the mold exit.

- Cracks form in steel while it is in the mold, or during secondary cooling prior to cropping. Sensors ideally should operate just before and just after secondary cooling so that the origin of cracking problems may be identified.
- Center looseness/porosity occur at the freeze-off point below the mold. A sensor to detect this phenomenon should be located at this point, provided it is known.

Question 3. Do internal discontinuities occur in higher concentrations during transient conditions (whether random disturbances or changes due to control action)? What transients are of importance? What discontinuities do they produce? Do we need sensors only when we change process conditions?

- There are three primary transient conditions that can cause internal discontinuities to occur in higher concentrations:
 1. At the beginning of the cast, the material behind the starter bar is unsound and must be cut off and discarded. The precise point of the transition of unsound material, containing a high incidence of impurities, is at present estimated (not measured).
 2. At any time, there is an equipment failure such as nozzle erosion spray nozzle stoppages or loss of stirring effectiveness.
 3. During the intermix zone during grade changes. In some cases, the process must be restabilized to a new operating point.
- The transient conditions above can impact internal cleanliness (with the introduction of both large and small inclusions with center line segregation), internal cracking and/or center looseness (porosity).

Since most upsets occur at random, it follows that a continuous scanning sensor is preferred. However, it is recognized that the size, orientation and types of internal discontinuities may, for some conditions, be predictable. For example, the starter bar and the intermix zones are known events. In each case, the types of internal discontinuities are known; therefore, the sensitivity requirements of sensing device may be different for these situations. Perhaps a study would be advantageous to rank the cost effectiveness of each sensing situation, and address collaborative program objectives on this as a priority.

Question 4. What benefits accrue from online detection of internal discontinuities? Can we quantify these benefits (% yield, % productivity, added product value)? How much should a sensor cost?

- Presently, no sensing/feedback control exists for production casters. Statistical process control (SPC) or quality management programs (QMP) are used to establish an operational "window" that results in the highest quality. Transients result in temporary excursions out of the window. Faults may also result in changes to the cooling system, flux efficiency, etc., that also take the caster outside its intended operational window. It may take days to weeks to recognize this.
- Internal discontinuity sensors could provide real-time indication of harmful excursion outside operational windows. Sensors with sufficient resolution/correct positioning could be a corner stone for narrowing the "window" and thus reducing caster operation costs, and improving the overall quality of material cast within window conditions.
- Considerable benefits are to be anticipated from the implementation of internal discontinuity sensors. These vary from caster to caster but nationwide could result in a 2% yield improvement.
- A sensor should "pay back" within six months to a year of implementation if it is to be economically justifiable in today's climate. Thus it must cost at least less than the value of a 1% yield improvement and preferably a factor of 3-5 less than this. Given the industry-wide need for such sensors, and their probable applicability to aluminum and other metal casters, a collaborative research program is probably called for in order to spread out research and development costs.

Question 5. what is the optimum sensor methodology for each class of internal discontinuity?

- Several sensor methodologies show promise. They include:
 1. Ultrasound
 2. Eddy currents
 3. X-ray tomography
- To achieve the spatial resolution needed in thick steel, x-ray tomography, would require very intense sources and numerous

detectors. Such a system could cost several millions of dollars unless emerging NDT systems can, in some way, be modified. Both ultrasonic and eddy current systems could be configured within the allowable cost range.

- Ultrasonic approaches are probably the best for center looseness, center line segregation, inclusions and some cracks. Traditional pulse-echo approaches fail for surface cracks but pitch-catch or surface wave techniques may be satisfactory. Eddy current methods show potential for surface crack problems but no other.

3.2 Intermediate Forming, Chairman, C.D. Rogers, U.S.S. Corporation, Recorder, M. Linzer, NBS.

Question 1. What are the internal discontinuities of importance during intermediate forming? Can they be prioritized on the basis of yield, controllability, etc? Are classes of internal discontinuity product specific?

- Three classes of defect should be detected. In order of priority they are:
 1. Subsurface inclusions greater than 150 μm located within 12.5 mm of the surface. These inclusions are mostly nonmetallics introduced in the molten metal prior to entry into the caster.
 2. Surface cracks greater than 12.5 mm depth and 150 mm long (after rolling).
 3. Subsurface inclusions and porosity with dimensions greater than 2.5 mm at depths greater than 150 mm. These defects can occur in almost any product. The surface defects can result in poor surface quality of strip product. Internal discontinuities can be particularly severe for defense specification grades and product destined for drawing/forming.

Question 2. What sensor methodologies are best suited to online detection of each class of internal discontinuity?

- Ultrasonic techniques show the best promise for detecting subsurface inclusions, cracks and porosity.
- Eddy current methods may prove useful for detecting surface cracks, though ultrasonics may be the preferred approach ultimately.

Question 3. What are the benefits accruing from online detection of internal discontinuities? Can these benefits be quantified (% yield, % productivity, added product value)? How much should a sensor cost?

- Optimized cropping/product diversion would maximize productivity while maintaining acceptable quality.
- 100% sensor inspection would provide valuable information about casting practices and could be fed back to optimize continuous casting practices.
- Optimized reduction to seal center looseness and avoid downstream quality problems during piercing, drawing and/or forming.

3.3 Finishing. Chairman, W. Wilson, Weirton Steel Corporation, Recorder, R.B. Clough, N.B.S.

Question 1. What are the internal discontinuities of importance during finishing? Can they be prioritized on the basis of yield, controllability, etc? Are classes of discontinuity product specific?

- The internal discontinuities of importance during finishing are inclusions, piping and center line cracking. These can be prioritized on the basis of yield, detectability, cost, controllability and the stage of manufacture. Because of all of these factors, the classes are usually product specific.

Question 2. What can be done when discontinuities are detected?

- The product can be accepted if it meets certain specifications which are a function of vendor and market conditions as well as production costs or rejected. It is desirable to reject such products as early in the production cycle as possible to reduce production costs. The level at which the product is rejected is critical and will depend on the technology of detection and economics of the specific situation. Early detection and remedial actions to upstream processes is the preferred strategy for quality improvement.

Question 3. What sensor methodologies are best suited to online detection of each class of internal discontinuity?

- Acoustic methods are best suited for thick steel sections. These methods are also more sensitive to internal discontinuities than radiographic methods, which do not provide good contrast for cracks

that are closed. Eddy current methods are limited to surface discontinuities.

Question 4. What benefits accrue from internal discontinuity detection during finishing operations? Can these benefits be quantified (% yield, % productivity, added product value)? How much should a sensor cost?

- The benefits of internal discontinuity detection at this stage of processing are not economic, at least in the short term, due to higher recycling costs and decreased productivity. Benefits accrue in the long term however, due to decreased customer dissatisfaction and enhanced quality.
- It is desirable to detect internal discontinuities prior to finishing operations to reduce production costs.
- A sensor ideally should not cost over \$1,000.

Question 5. Do other quantities (e.g., grain size) need to be measured during finishing?

- The consensus of the group was that these would not provide sufficiently useful information to justify costs. Unless such information were required for specification purposes, such measurements do not appear necessary.

U.S. DEPT. OF COMM. BIBLIOGRAPHIC DATA SHEET <i>(See instructions)</i>	1. PUBLICATION OR REPORT NO. NBSIR 88-3731	2. Performing Organ. Report No.	3. Publication Date JUNE 1988
4. TITLE AND SUBTITLE <p style="text-align: center;">Report of Workshop - Internal Discontinuity Sensor Needs for Steel</p>			
5. AUTHOR(S) <p style="text-align: center;">H. N. G. Wadley</p>			
6. PERFORMING ORGANIZATION <i>(If joint or other than NBS, see instructions)</i> <p style="text-align: center;">NATIONAL BUREAU OF STANDARDS U.S. DEPARTMENT OF COMMERCE GAITHERSBURG, MD 20899</p>			7. Contract/Grant No. 8. Type of Report & Period Covered
9. SPONSORING ORGANIZATION NAME AND COMPLETE ADDRESS <i>(Street, City, State, ZIP)</i> <p style="text-align: center;">The American Iron and Steel Institute 1133 15th St. N.W. Washington D. C. 20005</p>			
10. SUPPLEMENTARY NOTES <input type="checkbox"/> Document describes a computer program; SF-185, FIPS Software Summary, is attached.			
11. ABSTRACT <i>(A 200-word or less factual summary of most significant information. If document includes a significant bibliography or literature survey, mention it here)</i> <p>Operators, engineers and researchers representing American Iron and Steel Institute member companies met with scientists and engineers from federal laboratories, universities and sensor vendor companies to determine the formation mechanisms of internal discontinuities in continuous cast steel, identify sensors for their detection and control strategies for their elimination.</p> <p>The development of online sensors to detect inclusions and cracks within the caster was determined to be urgently needed for real time quality control. Outputs from such sensors could be used to detect inert gas shroud cracking (the most common source of the most deleterious inclusions) and cracking problems and facilitate feedback control. Of all the potential sensor methodologies addressed, ultrasonic approaches similar to those developed for porosity work and also related to those under development for internal temperature/solidification interface measurement were considered the most promising. Collaborative programs need to be instituted to prove the ultrasonic approach and develop data for the design of a prototype sensor.</p>			
12. KEY WORDS <i>(Six to twelve entries; alphabetical order; capitalize only proper names; and separate key words by semicolons)</i> <p>continuous casting; eddy currents; inclusions; porosity; solidification; ultrasonics.</p>			
13. AVAILABILITY <input checked="" type="checkbox"/> Unlimited <input type="checkbox"/> For Official Distribution. Do Not Release to NTIS <input type="checkbox"/> Order From Superintendent of Documents, U.S. Government Printing Office, Washington, D.C. 20402. <input checked="" type="checkbox"/> Order From National Technical Information Service (NTIS), Springfield, VA. 22161			14. NO. OF PRINTED PAGES <p style="text-align: center;">70</p> 15. Price <p style="text-align: center;">\$13.95</p>

